# Extracting abundance information from DNA-based data

Mingjie Luo[1,2], Yinqiu Ji[1], Douglas W. Yu[1,3,4]

[1] State Key Laboratory of Genetic Resources and Evolution and Yunnan Key Laboratory of Biodiversity and Ecological Security of Gaoligong Mountain, Kunming Institute of Zoology, Chinese Academy of Sciences, Kunming, Yunnan, China 650223
[2] Kunming College of Life Sciences, University of Chinese Academy of Sciences, Kunming, China
[3] Center for Excellence in Animal Evolution and Genetics, Chinese Academy of Sciences, Kunming Yunnan, China 650223
[4] School of Biological Sciences, University of East Anglia, Norwich Research Park, Norwich, Norfolk, UK NR47TJ

## Abstract

The accurate extraction of species-abundance information from DNA-based data (metabarcoding, metagenomics) could contribute usefully to diet reconstruction and quantitative food webs, the inference of species interactions, the modelling of population dynamics and species distributions, the biomonitoring of environmental state and change, and the inference of false positives and negatives. However, capture bias, capture noise, species pipeline biases, and pipeline noise all combine to inject error into DNA-based datasets. We focus on methods for correcting species pipeline biases and pipeline noise, as the first two errors are addressed extensively in the ecological literature. To extract abundance information, it is useful to distinguish two concepts. (1) *Across*-species quantification describes relative species abundances within one sample. (2) *Within*-species quantification describes how the abundance of each individual species varies from sample to sample, as in a time series, an environmental gradient, or different experimental treatments. Firstly, we review methods to remove species pipeline biases and pipeline noise. Secondly, we demonstrate experimentally (with a detailed protocol) how to use a 'DNA spike-in' or 'Unique Molecular Identifiers' (UMIs) to remove pipeline noise and recover within-species abundance information.

## Introduction

The accurate extraction of species-abundance information from DNA-based data could contribute usefully to the reconstruction of diets and quantitative food webs, the inference of species interactions, the modelling of population dynamics and species distributions, the biomonitoring of environmental state and change, and more prosaically, the inference of false positives and negatives (Thomas et al. 2016; Deagle et al. 2019; Peel et al. 2019;

Carraro et al. 2020, 2021; Abrego et al. 2021; Rojahn et al. 2021). *Here we use the term abundance to mean any estimate of biomass or count of individuals*.

However, there are four general obstacles to the extraction of abundance information from DNA-based data (see Shelton et al. 2016; Griffin et al. 2020 for more formal treatments), which we will call here: (1) *species capture biases*, (2) *capture noise*, (3) *species pipeline biases*, and (4) *pipeline noise*.

1. *Species capture biases*. – Different species are more or less likely to be captured by a given sampling method or via non-random sampling designs. For instance, Malaise traps preferentially capture Diptera (deWaard et al. 2019), and different fish species, body sizes, and physiological conditions vary in their eDNA shedding rates (Thalinger et al. 2021; Yates et al. 2021*b*).
2. *Capture noise*. – Steinke et al. (2021) have shown that Malaise traps separated by only 3 m fail to capture the same species compositions, from which we infer that abundances vary stochastically across traps. Levi et al. (2019) showed that counts of salmon could be estimated via quantitative PCR of aquatic environmental DNA, but only after correcting for temporal fluctuations in streamflow. Other sources of capture noise include environmental variation in eDNA degradation rates, food availability, PCR inhibitors, and transport rates (reviewed in Yates et al. 2021*a*).
3. *Species pipeline biases*. – Species differ in body size (biomass bias), genome size, mitochondrial copy number, DNA extraction efficiency, and PCR amplification efficiency (primer bias) (Amend et al. 2010; Yu et al. 2012; Elbrecht and Leese 2015; Piñol et al. 2015, 2019; Tang et al. 2015; Bell et al. 2017; Krehenwinkel et al. 2017; McLaren et al. 2019; Pauvert et al. 2019; Garrido-Sanz et al. 2021; Yang et al. 2021). Species can even differ in their propensity to survive a bioinformatic pipeline, such as when closely related species are clustered into one operational taxonomic unit (Pauvert et al. 2019).
4. *Pipeline noise*. – There is considerable noise in DNA-based pipelines, which breaks the relationship between starting sample biomasses and final numbers of reads per sample (Ji et al. 2020), caused in part by PCR stochasticity and the passing and pooling of small aliquots of liquid along wet-lab pipelines. In particular, it is common practice *to deliberately equalise the amount of data per sample* by “pooling samples in equimolar concentration” just before sequencing.

We do not consider species capture biases or capture noise further, referring the reader to the literature on eDNA occupancy correction (e.g. Dorazio and Erickson 2018; Doi et al. 2019; Erickson 2019; Griffin et al. 2020; Lyet et al. 2021; Stauffer et al. 2021) and the review by Yates et al. (2021*a*). Instead, our purpose is to review methods for the extraction of

abundance information from already-collected samples, because even if species capture biases and capture noise can be corrected, the combination of species pipeline biases and pipeline noise still *causes the number of DNA sequences assigned to a species in a sample to be an error-prone measure of the abundance of that species in that sample* (McLaren et al. 2019).

To start, we illustrate in a simplified way how pipeline noise and species pipeline biases (hereafter, species biases) combine to inject error into DNA-based datasets. We start with a notionally true sample X species table or OTU table (Figure 1), where OTU stands for Operational Taxonomic Unit, i.e. a species hypothesis. Let each cell represent the true abundance (biomass or count) of that OTU in that sample.

Pipeline noise affects the *rows* (samples) of an OTU table. Thus, even though in the true table, OTU1 is six times as abundant in sample 4 versus sample 1 (green cells in Figure 1 A), in the observed table, OTU1 is only *two* times as abundant in sample 4 (green cells in Figure 1 B). *Pipeline noise thus obscures how the abundance of each individual species varies across samples, where the samples could be a time series, an environmental gradient, or different experimental treatments*.

Species bias affects the *columns* (OTUs) of an OTU table. Thus, even though in the true table, OTU2 and OTU1 are equally abundant in sample 3 (orange cells in Figure 1 A), in the observed OTU table, OTU2 is two times as abundant as OTU1 in sample 3 (orange cells in Figure 1 B). Species bias thus obscures *relative species abundances*, which is important for diet analysis (Deagle et al. 2019) and when relative abundance within a sample provides information on species contribution to ecosystem functioning or services (e.g. relative fish species biomasses).

So how can we extract abundance information from DNA-based data? It is helpful to distinguish between two concepts from Ji et al. (2020; see also Garrido-Sanz et al. 2021):

1. *Within*-species (across-sample) quantification: E.g. “Species A is more abundant in this sample than it is in that sample (e.g. two points on a time series).” This is achieved by removing pipeline noise (Figure 2 A1, D).
2. *Across*-species (within-sample) quantification: E.g. “Species A is more abundant than Species B *in this sample* (i.e. relative species abundance).” This is achieved by removing species biases.

As we review and demonstrate below, some approaches remove pipeline noise, some remove species biases, and some remove both. *Our take-home message is that removing only pipeline noise to achieve within-species quantification can be enough* to improve the inference of species interactions, the modelling of population dynamics and species

distributions, the biomonitoring of environmental state and change, (Carraro et al. 2020, 2021; Abrego et al. 2021; Rojahn et al. 2021), and the inference of false positives and negatives (Figure 3).

*Mini-review of methods to extract abundance information*

*Multiplexed individual barcoding*. – The most straightforward approach is to DNA-barcode individual organisms and count them up, which achieves both within- and across-species quantification. This approach assumes bulk samples, with a target taxon (e.g. Insecta) that has body sizes suitable for mass individual sorting. DNA extraction, uniquely tagged PCR, and subsequent pooling and sequencing on an Illumina (Meier et al. 2016; Ratnasingham 2019; Creedy et al. 2020), PacBio (Hebert et al. 2018), or MinION (Srivathsan et al. 2021) now costs much less than $1 per individual. Wührl et al. (2021) further increase throughput with a robotic pipettor and camera that visually IDs small insects to higher taxonomic rank and sorts them into 96-well plates for individual DNA barcoding. This method achieves both within- and across-species quantification but is difficult to apply to very large numbers of samples and cannot be applied to trace DNA or microbial taxa.

*Presence-absence in multiple subsamples*. – Presence-absence across multiple subsamples can be used as an index of abundance. For instance, Abrego et al. (2021) summed all weekly detections (presences) per species in their mitogenomic arthropod dataset to estimate an annual abundance measure for each species. However, the optimal number of subsamples needs to be determined in order to be able to 'count' species of varying abundances (common or rare), and adding many subsamples increases cost. This method can achieve partial within-species quantification but probably not across-species quantification.

*Design better PCR primers*. – In some cases, the target taxon is nearly uniform in body size and DNA-extraction efficiency, and it can be possible to design PCR primers that bind similarly across species. For instance, Schenk et al. (2019) have reported that primers for the 28S D3-D5 and 18S V4 regions return nematode read frequencies that accurately recover relative species abundances. Similarly, Verkuil et al. (2020) have reported that modified COI primers can recover the relative biomasses of insect orders from Pied Flycatcher faeces. This method achieves across-species quantification but not within-species quantification.

*Quantitative/Digital-Droplet PCR*. – qPCR and ddPCR (quantitative and digital droplet PCR) can be used to estimate the sample DNA concentration of one species per assay. ddPCR is more sensitive than is qPCR (Brys et al. 2021) and allows the detection of single copies of target DNA and absolute quantification through the partitioning of the PCR reaction into 20,000 droplets and subsequent fluorescent detection of droplets that contain the target DNA

(Hindson et al. 2011). This paper does not review q/ddPCR except to note that single-species q/ddPCR applied to aquatic trace DNA can estimate absolute abundances, provided that one corrects for water flux and/or surface-area to mass ratio (Levi et al. 2019; Pochardt et al. 2020; Fukaya et al. 2021; Yates et al. 2021*b*, 2021*a*). If applied to multiple species and if statistical models that relate DNA copy number to abundance can be fitted (Levi et al. 2019; Pochardt et al. 2020; Fukaya et al. 2021), then across-species quantification can also be achieved, albeit with non-trivial amounts of error.

*Spike-in DNA.* – To achieve within-species quantification, researchers have advocated adding a fixed amount of an arbitrary DNA sequence to each sample, after tissue lysis and before DNA extraction, also known as an internal standard (ISD, Harrison et al. 2021). The 'spike-in' sequence of course should not match any species that could be in the samples and is flanked by primer binding sequences that match the primers used (Smets et al. 2016; Deagle et al. 2018; Tkacz et al. 2018; Harrison et al. 2021). Because each sample receives the same amount of spike-in, all samples should in theory return the same number of spike-in reads, but pipeline noise ensures that this never happens. Some samples return more spike-in reads, meaning that their OTUs are too large (too many reads), and some samples return fewer spike-in reads, meaning that their OTUs are too small. The correction step is simple: divide each sample's OTU sizes by the number of spike-in reads in that sample (Ji et al. 2020; Abrego et al. 2021) or include the spike-in reads as an offset term in a multivariate statistical model (Wang et al. 2012). Samples with a high number of spike-in reads must have had a low amount of template DNA, and vice versa, so dividing shrinks OTU sizes accordingly. For instance, following the pioneering work of Zhou et al. (2013), Ji et al. (2020) mapped WGS datasets of insects to mitochondrial genomes and barcodes and achieved nearly perfect within-species quantification (barcodes $R^2$ = 93%, mitogenomes $R^2$ = 95%) and almost direct proportionality between mapped reads and input DNA-mass. The high accuracy was achieved by employing a spike-in, replicates to correct for sequence-run noise (an additional source of pipeline noise), and a percent-coverage filter to remove false positives. However, the regression lines relating read number to input DNA for each species all had different intercepts, reflecting uncorrected species biases, and thus across-species quantification was not achieved. Harrison et al. (2021) provide an excellent, complementary review of the recent literature on spike-ins and also describe an alternative approach for modelling non-spike-corrected ('compositional') datasets.

*Unique Molecular Identifiers (UMIs).* – A UMI is a series of ~7-12 random bases ('NNNNNNN') added to the forward primer as an ultra-high diversity tag (Hoshino and Inagaki 2017). Seven Ns produce $4^7$ = 16 384 uniquely identified forward primer molecules. Species contributing abundant DNA to a sample will capture many of these primer molecules

and thus amplify many unique UMIs, while species contributing scarce DNA will amplify a low number. The relationship between UMI richness and DNA abundance is roughly linear but asymptotes for species with very high DNA abundance. After sequencing, the number of UMIs per OTU correlates with the starting number of template DNA molecules per species in that sample (Hoshino and Inagaki 2017; Hoshino et al. 2021). This method thus mimics q/ddPCR in that if statistical relationships between DNA copy number and true abundance can be estimated, across-species quantification can be achieved. Within-species quantification can be achieved by also adding a spike-in.

*Multiview modelling*. – Williamson et al. (2021) have proposed a method for achieving across-species quantification. Originally, McLaren et al. (2019) pointed out that although it is not possible to estimate *a priori* the species biases in a given amplicon or metagenomic dataset (because an unknown number of factors of unknown strengths combine to create the biases), it is reasonable to assume that *the ratio of the biases of every pair of species is fixed*. Thus, if one first estimates the absolute abundances of a subset of species in the dataset (via multiple, species-specific q/ddPCR assays), it is possible to infer the absolute abundances of the rest of the species (by inferring from data their ratios with the q/ddPCR-quantified species), allowing one to achieve across-species quantification. The authors dub this a 'multiview data structure' because there are two views into the community of interest: q/ddPCR and sequencing. Note that because q/ddPCR is carried out after many of the wet-lab steps have been carried out, multiview modelling does not remove pipeline noise. Thus, a spike-in is still needed to achieve within-species quantification.

*Forward and reverse metagenomics*. – Lang et al. (2019) showed that WGS (whole-genome sequencing) datasets from pollen samples mapped to the variable protein-coding regions in chloroplast genomes can achieve accurate across-species quantification, finding that read frequency correlated strongly and linearly with pollen-grain frequency in a nearly 1:1 relationship ($R^2$ = 86.7%, linear regression). At the same time, Peel et al. (2019) showed that it is possible to skip the labour of assembling and annotating chloroplast genomes, by using long-read sequences produced by the MinION sequencers from Oxford Nanopore Technologies (ONT). In this protocol, unassembled genome skims of individual plant species, ideally sequenced at ≥1.0X depth, are used as reference databases. Mixed-species query samples of pollen are sequenced on MinIONs. The reads from each (reference) genome skim are mapped to each (query) long read, and each long read is assigned to the species whose skim maps at the highest percent coverage. This 'reverse metagenomic' (RevMet) protocol achieves across-species quantification, allowing biomass-dominant species to be identified in mixed-species pollen samples (and potentially, in root masses). Because RevMet uses the whole genome, it avoids species biases and pipeline noise

created by ratios of chloroplasts to cells varying across species, condition, tissues, and age, and it can potentially be applied to any taxon for which it is possible to generate large numbers of individual genome skims, potentially including soil fauna. However, metagenomics by itself does not remove pipeline noise and would have to be paired with a spike-in to achieve within-species quantification.

To sum up, multiple methods exist to extract abundance information from DNA-based datasets. Some achieve within-species quantification (by removing pipeline noise), some achieve across-species quantification (by removing species biases), and some achieve both or can be combined to achieve both. However, many ecological questions can be answered by achieving only within-species quantification (Figure 3), and in the second half of this paper, we provide a detailed protocol and experimental validation for spike-ins to achieve within-species quantification.

A. True OTU table

| | OTU1 | OTU2 | OTU3 | OTU4 | spikeOTU | True rowSum |
|---|---|---|---|---|---|---|
| Sample 1 | 10 | 20 | 0 | 0 | 20 | **30** |
| Sample 2 | 0 | 100 | 20 | 50 | 20 | **170** |
| Sample 3 | 40 | 40 | 5 | 50 | 20 | **135** |
| Sample 4 | 60 | 0 | 30 | 100 | 20 | **190** |

scales::rescale() each OTU (column) to interval [0,1]

A1. True OTU table, each OTU rescaled to [0,1]

| | OTU1 | OTU2 | OTU3 | OTU4 |
|---|---|---|---|---|
| Sample 1 | 0.2 | 0.2 | 0.0 | 0.0 |
| Sample 2 | 0.0 | 1.0 | 0.7 | 0.5 |
| Sample 3 | 0.7 | 0.4 | 0.2 | 0.5 |
| Sample 4 | 1.0 | 0.0 | 1.0 | 1.0 |

Metabarcoding or metagenomic pipeline

Within-OTU (within-column) frequencies recovered by spike-correction

B. Observed OTU table with pipeline noise and species pipeline biases

| | OTU1 | OTU2 | OTU3 | OTU4 | spikeOTU | Pipeline noise | Observed rowSum |
|---|---|---|---|---|---|---|---|
| Sample 1 | 30 | 120 | 0 | 0 | 90 | 3 | **150** |
| Sample 2 | 0 | 600 | 240 | 900 | 90 | 3 | **1740** |
| Sample 3 | 80 | 160 | 40 | 600 | 60 | 2 | **880** |
| Sample 4 | 60 | 0 | 120 | 600 | 30 | 1 | **780** |
| Species biases | 1 | 2 | 4 | 6 | 1.5 | | |

DNA spike-in correction

divide each row by its spikeOTU

C. Spike-corrected OTU table

| | OTU1 | OTU2 | OTU3 | OTU4 |
|---|---|---|---|---|
| Sample 1 | 0.3 | 1.3 | 0.0 | 0.0 |
| Sample 2 | 0.0 | 6.7 | 2.7 | 10.0 |
| Sample 3 | 1.3 | 2.7 | 0.7 | 10.0 |
| Sample 4 | 2.0 | 0.0 | 4.0 | 20.0 |
| | 1 | 2 | 4 | 6 |

scales::rescale()

D. Spike-corrected OTU table, each OTU rescaled to [0,1]

| | OTU1 | OTU2 | OTU3 | OTU4 |
|---|---|---|---|---|
| Sample 1 | 0.2 | 0.2 | 0.0 | 0.0 |
| Sample 2 | 0.0 | 1.0 | 0.7 | 0.5 |
| Sample 3 | 0.7 | 0.4 | 0.2 | 0.5 |
| Sample 4 | 1.0 | 0.0 | 1.0 | 1.0 |

mvabund::manyglm(OTUtable ~ 1 + offset(log(spikeOTU)))

otu[otu>0] <- 1

otu[otu>0] <- 1

E. Presence-Absence OTU table

| | OTU1 | OTU2 | OTU3 | OTU4 |
|---|---|---|---|---|
| Sample 1 | 1 | 1 | 0 | 0 |
| Sample 2 | 0 | 1 | 1 | 1 |
| Sample 3 | 1 | 1 | 1 | 1 |
| Sample 4 | 1 | 0 | 1 | 1 |

F. Observed OTU table, divided by Observed rowSum

| | OTU1 | OTU2 | OTU3 | OTU4 |
|---|---|---|---|---|
| Sample 1 | 0.2 | 0.8 | 0.0 | 0.0 |
| Sample 2 | 0.0 | 0.3 | 0.1 | 0.5 |
| Sample 3 | 0.1 | 0.2 | 0.0 | 0.7 |
| Sample 4 | 0.1 | 0.0 | 0.2 | 0.8 |
| Species biases | 1 | 2 | 4 | 6 |

G. Observed OTU table, divided by Observed rowSum, each OTU rescaled to [0,1]

| | OTU1 | OTU2 | OTU3 | OTU4 |
|---|---|---|---|---|
| Sample 1 | 1.0 | 1.0 | 0.0 | 0.0 |
| Sample 2 | 0.0 | 0.4 | 0.9 | 0.7 |
| Sample 3 | 0.5 | 0.2 | 0.3 | 0.9 |
| Sample 4 | 0.4 | 0.0 | 1.0 | 1.0 |
| Species biases | 1 | 2 | 4 | 6 |

**Figure 1**. **Pipeline noise versus species bias in OTU tables**. **A**. The true OTU table, with cell numbers representing the true amounts of DNA or biomass for each OTU (column) in each sample (row). The true rowSum column thus shows the total DNA or biomass per sample, and the spikeOTU column shows that the same amount of standard DNA spike-in has been added to each sample. **A1**. The true OTU table after rescaling each OTU column to the interval [0,1] ('quasiprobabilities'). **B**. The observed OTU table after amplicon or shotgun sequencing, showing the combined effects of pipeline noise and species biases. Each cell in Table A is multiplied by the Pipeline noise and Species bias values in that cell's row and column. Pipeline noise causes the original 10:60 ratio of Sample 1 and Sample 4 in OTU1 (green cells) to appear as 30:60, and species bias causes the original 40:40 ratio of OTU1 and OTU2 (orange cells) to appear as 80:160. **C**. The observed OTU table after dividing each row by the observed spike-in reads, to remove pipeline noise. **D**. Table C after rescaling each OTU column to the interval [0,1], to allow direct comparison with the rescaled true-OTU Table A1. Spike-in correction successfully recovers *within-species* abundance change from sample to sample. In statistical modelling, observed spike-in values are an index of sampling (sequencing) effort and can be included as offset values. **E**. If spike-in reads are not available, or if it is suspected that capture noise is uncorrectable and high, the observed OTU table can be transformed to presence/absence. However, this method potentially loses ecological information (**Figure 3**). **F.** Pipeline noise cannot be reliably removed by using the total reads per sample as a proxy for sampling effort (Observed rowSum) because the observed rowSum is confounded by species composition. **G**. Table 4 after rescaling each OTU column to the interval [0,1], to contrast with Tables A1 and D. Line graphs of the OTU tables are in **Figure 2**. Code syntax from the R language (R Core Team 2021), including the {mvabund} (Wang et al. 2012) and {scales} packages (https://scales.r-lib.org, accessed 16 Dec 2021). (**353 words**)

**Figure 2**. **Line graphs of Figure 1, transposed so that each line is a column from the corresponding OTU table**. With spike-in correction, *within*-species abundance information is recovered (follow each OTU's line from sample to sample), but *across*-species abundance information is not (compare species abundances within each sample). Blue borders indicate that within-species abundance information has been preserved by using spike-in correction. Red borders indicate the loss of within-species abundance information. (**71 words**)

A. Absolute abundance data for one species

| | | |
|---|---|---|
| | | 3 |
| 3 | 30 | 3 |
| 3 | 21 | |
| 3 | 3 | 3 |

B. Within-species abundance data, [0,1]

| | | |
|---|---|---|
| | | 0.1 |
| 0.1 | 1 | 0.1 |
| 0.1 | 0.7 | |
| 0.1 | 0.1 | 0.1 |

C. Presence-absence data for one species

| | | |
|---|---|---|
| | | 1 |
| 1 | 1 | 1 |
| 1 | 1 | |
| 1 | 1 | 1 |

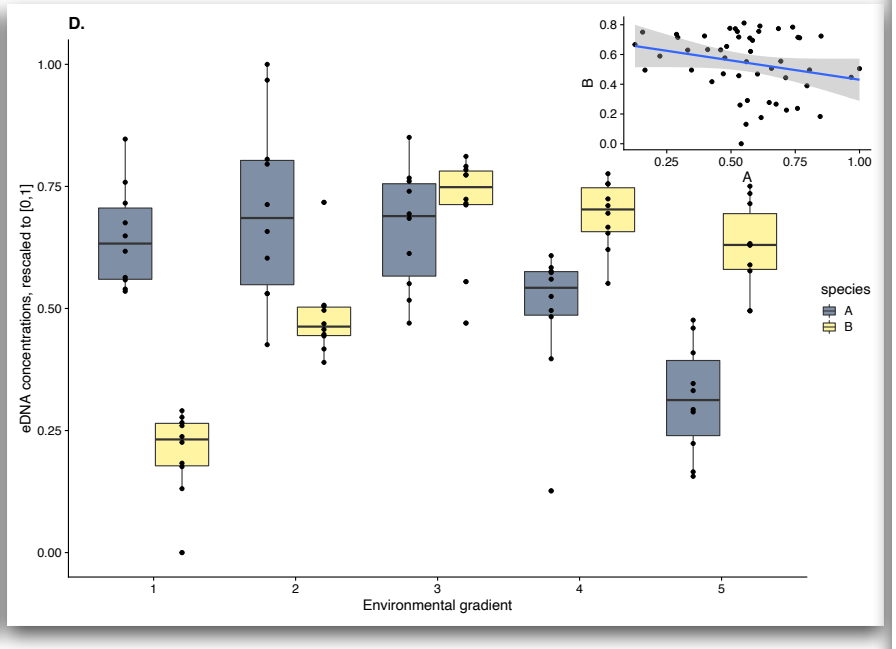


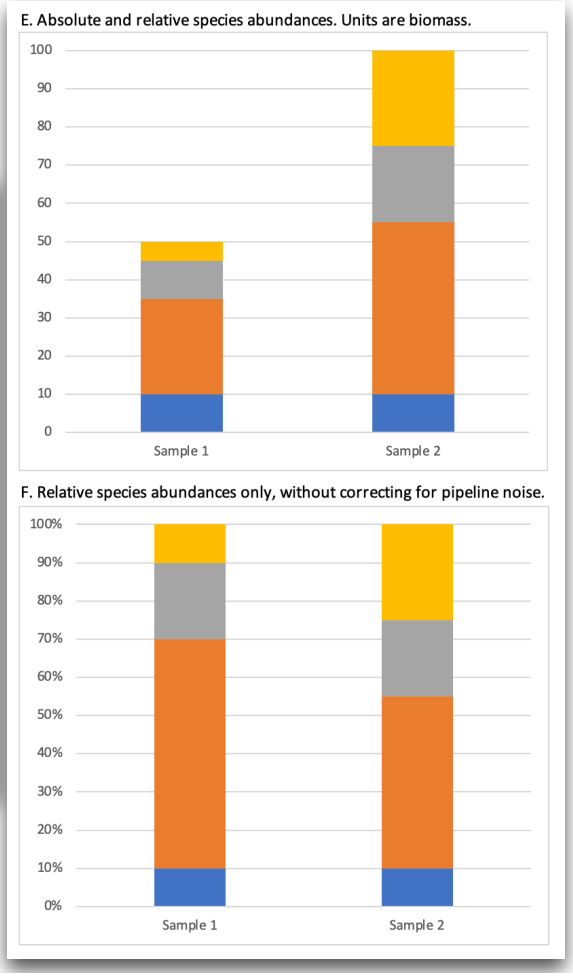


**Figure 3**. **The usefulness of achieving only within-species or only across-species quantification**. **A.** Imagine that a species is found in many sites but that only two sites are optimal (green) with high abundances, while most sites are suboptimal (grey) with low abundances maintained by immigration. **B**. Let the existence of unquantified species biases make it impossible to recover absolute abundances from DNA-based data, but as long as pipeline noise is removed with a spike-in, it is still possible to track how the species' abundance varies across sites (rescaled to [0,1]), which generates the hypothesis that the green sites are optimal habitat. **C**. If the DNA-based data were converted to presence/absence, the distinction

between green and grey habitat would be lost. **D**. Along an environmental gradient from left to right, species A decreases, and species B increases in eDNA concentration. Even without correcting for species biases, removal of pipeline noise (and capture noise) allows the detection of a negative correlation in abundances (inset). Example adapted from Rojahn et al. (2021) who combined a similar result with external information to infer the competitive exclusion of a native fish species by an invasive species. Note that due to species biases, it is not possible to infer from these within-species abundance gradients which species is more abundant than the other (nor is it correct to infer that the two species are of similar abundance). **E**. Two samples with different absolute and relative species abundances. **F**. If only across-species quantification is achieved (e.g. via forward or reverse metagenomics), it is only valid to compare across species *within* a sample. Thus, it is valid to conclude that the dark orange species has the highest relative abundance in both samples 1 and 2, but it is not valid to conclude that the dark orange species has a greater biomass in Sample 1 than in Sample 2, as can be seen by inspection of the true absolute abundances in **E**. However, adding a spike-in and also achieving within-species quantification would recover total biomasses and make it possible to compare how each species' abundances vary across samples (E). (**349 words**)

## Methods

*2.1 Mock soup construction.* – 286 arthropods were collected in Kunming, China (25°8'23" N, 102°44'17" E). DNA was extracted from each individual using the DNeasy Blood & Tissue Kit (Qiagen GmbH, Germany). Genomic DNA concentration of each individual was quantified from three replicates using PicoGreen fluorescent dye. 658-bp COI barcoding sequences were PCRd with Folmer primers (LCO1490 and HCO2198) and Sanger-sequenced. After the 658-bp COI sequences were trimmed to 313 bp based on our metabarcoding primers (see below), 286 arthropods were clustered to 168 OTUs at 97% similarity. We selected 52 individuals with genomic DNA > 20 ng/µl, representing 52 OTUs. Each mock soup was constructed with equal masses of purified genomic DNA from the 52 OTUs. Input genomic DNA masses of each OTU from soup 1 to soup 7 decreased by 0.8X to create seven mock soups of differing absolute abundances. Each of the seven soups was made in triplicate ($n_{tot}$ = 21) (Figure 4 A).

*2.2 Preparation of Malaise-trap samples.* – 244 Malaise-trap samples from 96 sites, using 99.9 % ethanol as the trapping liquid, were collected in and near a 384 $km^2$ forested landscape containing the H.J. Andrews Experimental Forest (44.2° N, 122.2° W), Oregon, United States in July 2018. Traps were left for 7 non-rainy days. To equalize biomass across individuals, we only kept the heads of large individuals (body lengths >2 cm) and then transferred the samples to fresh 99.9% ethanol to store at room temperature until extraction. The samples were air dried individually on filter papers for less than an hour and then transferred to 50 ml tubes or 5 ml tubes according to sample volume. The samples were then weighed. DNA was non-destructively extracted by soaking the samples in lysis buffer, using the protocol from Ji et al. (2020) and Nielsen et al. (2019). For this study, we selected seven samples spread over the study area. After completion of lysis, we serially diluted the 7 samples by using 0.7X lysis buffer volume (500 µl, 350 µl, 245 µl, 171.5 µl, 120 µl and 84 µl) to create six soups per sample ($n_{tot}$ = 42). We used QIAquick PCR purification kit (Qiagen GmbH, Germany) following the manufacturer instructions to purify lysis buffer on one spin column per soup (Figure 4 B).

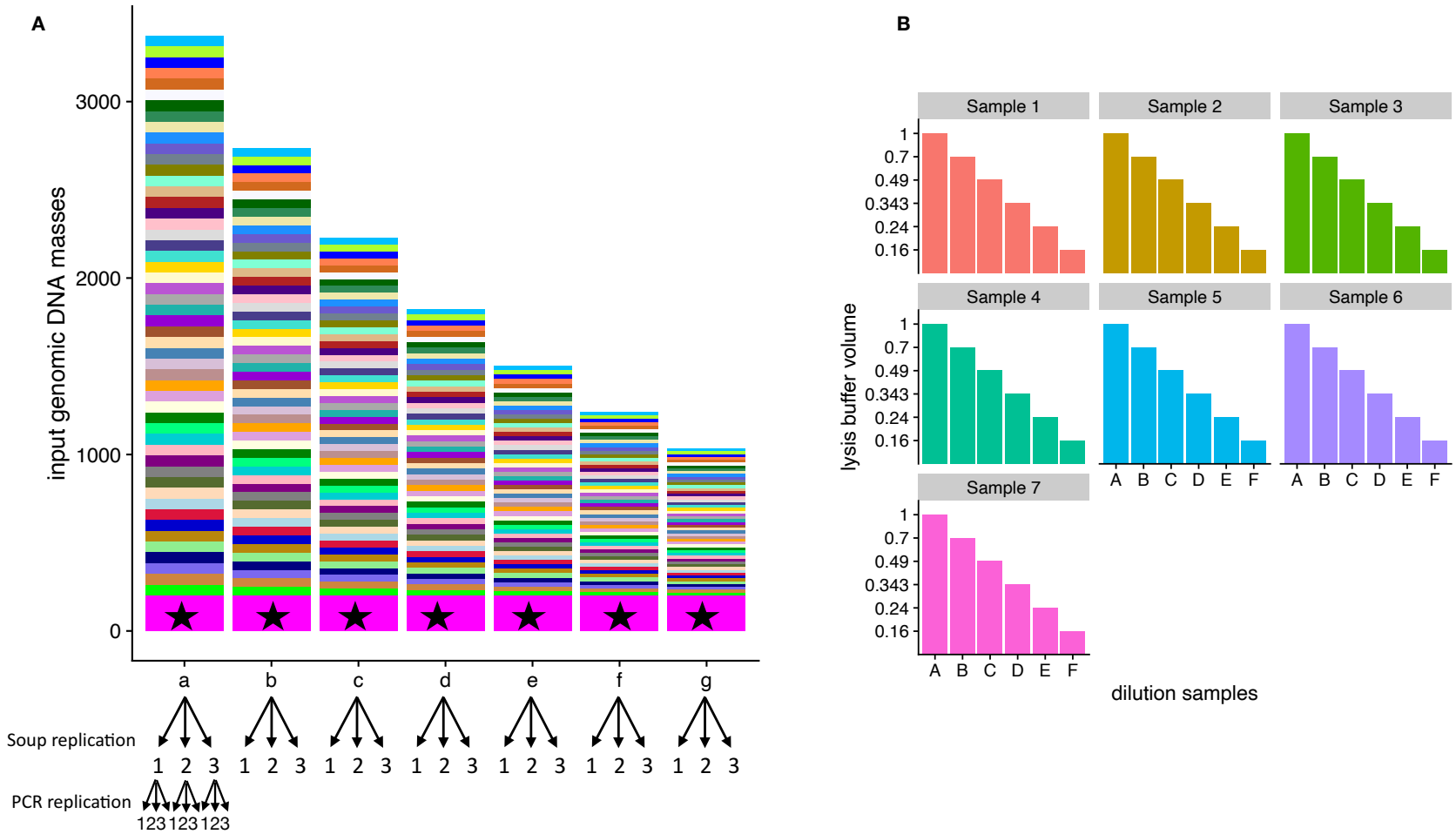


**Figure 4**. **Preparation of mock and Malaise-trap soups**. A. Mock soups. Each mock soup was constructed with equal masses of purified DNA from 52 OTUs. From soup "a" to soup "g", the input genomic masses of each of the 52 OTUs were 61, 48.8, 39, 31.2, 25, 20 and 16 ng. The same mass of spike-in DNA was then added to each soup (star). Each of the seven soups was made in triplicate, and all 21 soups were PCR'd in triplicate following the Begum pipeline (Yang et al. 2021) to detect and remove false reads. B. Malaise-trap soups. 500 µl, 350 µl, 245 µl, 171.5 µl, 120 µl and 84 µl of lysis buffer were used to create 6 soups (A-F) per sample. The spike-in DNA was added before extraction. Each soup ($n_{tot}$ = 42) was PCR'd in triplicate. (**139 words**)

296 *2.3 Adding spike-in DNA*

297 *2.3.1 Spike-in DNA.* – For our spike-ins, we used three insect species from China
298 (Lepidoptera:Bombycidae, Coleoptera:Elateridae, Coleoptera:Mordellidae), none of
299 which is expected to appear in the Oregon Malaise-trap samples. An alternative is to
300 use one or more synthetic, random DNA sequences (Tkacz et al. 2018). Each of our
301 three spike-ins is represented by a 658-bp COI fragment (Table 1) with primer binding
302 sites that match the Folmer primers HCO2198 and LCO1490. For long-term storage,
303 we inserted the COI fragments as plasmids into monoclonal bacteria. Plasmids were
304 extracted using TIANprep Mini Plasmid Kit (Beijing, China) following manufacturer's
305 instructions.

306 *2.3.2 Adding spike-in to the mock soups.* – Adding too much spike-in wastes
307 sequencing data, while adding too little risks loss of abundance information in at least
308 some samples when the number of spike-in reads is too low to use as a reliable
309 correction factor. Thus, we quantified the COI copy numbers of the mock soups and
310 the spike-in DNA by qPCR, and chose a volume so that spike-in reads should make up
311 1% of the total number of COI copies in the lowest-concentration mock soups,
312 balancing efficiency with reliability. We used all three spike-in species here and mixed
313 them (Bombycidae:Elateridae:Mordellidae) in a ratio of 1:2:4, which was added directly
314 to the mock soups' DNA since they were already purified.

315 2.3.3 *Adding spike-in to the Malaise-trap samples.* – From the 244 Malaise-trap
316 samples, we first extracted 17 Malaise-trap samples without adding spike-ins, and then
317 we used qPCR to quantify the mean COI concentrations of these 17 samples in order
318 to decide how much spike-in to add. Before adding the spike-ins, we discovered that
319 the Bombycid DNA spike-in had degraded, and so we used only two spike-in species
320 for the Malaise trap samples, at a ratio of 1:9 (Mordellidae:Elateridae). For the 7
321 samples used in this study, lysis buffer (500 µl, 350 µl, 245 µl, 171.5 µl, 120 µl, 84 µl)
322 from each sample was transferred into clean 1.5 ml tubes, and the spike-in DNA was
323 added. We then purified the DNA with the Qiagen QIAquick PCR purification kit,
324 following the manufacturer instructions. DNA was eluted with 200 µl of elution buffer. In
325 this way, the spike-in DNA was co-purified, co-amplified, and co-sequenced along with
326 the sample DNA (Figure 5). We also recorded the total lysis buffer volume of each
327 sample, for downstream correction.

328 *2.4 Primer design.* – For this study, we simultaneously tested two methods for
329 extracting abundance information: spike-ins and UMIs (Unique Molecular Identifiers).
330 UMI tagging requires a two-step PCR procedure (Lundberg et al. 2013; Hoshino and
331 Inagaki 2017), first using tagging primers and then using amplification primers (Figure

332 6). The tagging primers include (1) the Leray-FolDegenRev primer pair to amplify the
333 313-bp COI amplicon of interest, (2) a 1- or 2-nucleotide heterogeneity spacer on both
334 the forward and reverse primers to increase sequence entropy for the Illumina
335 sequencer, (3) the same 6-nucleotide sequence on both the forward and reverse
336 primers to 'twin-tag' the samples for downstream demultiplexing, (4) a 5N random
337 sequence on the forward primer and a 4N random sequence on the reverse primer (9N
338 total) as the UMI tags, (5) and parts of the Illumina universal adapter sequences to
339 anneal to the 3' ends of the forward and reverse primers for the second PCR. By
340 splitting the 9N UMI into 5N + 4N over the forward and reverse primers, we avoid
341 primer dimers. The amplification primers include (1) an index sequence on the forward
342 primer pair for Illumina library demultiplexing, and (2) the full length of the Illumina
343 adapter sequences. For further explanation of the design of the tagging primers (except
344 for the UMI sequences), see Yang et al. (2021).

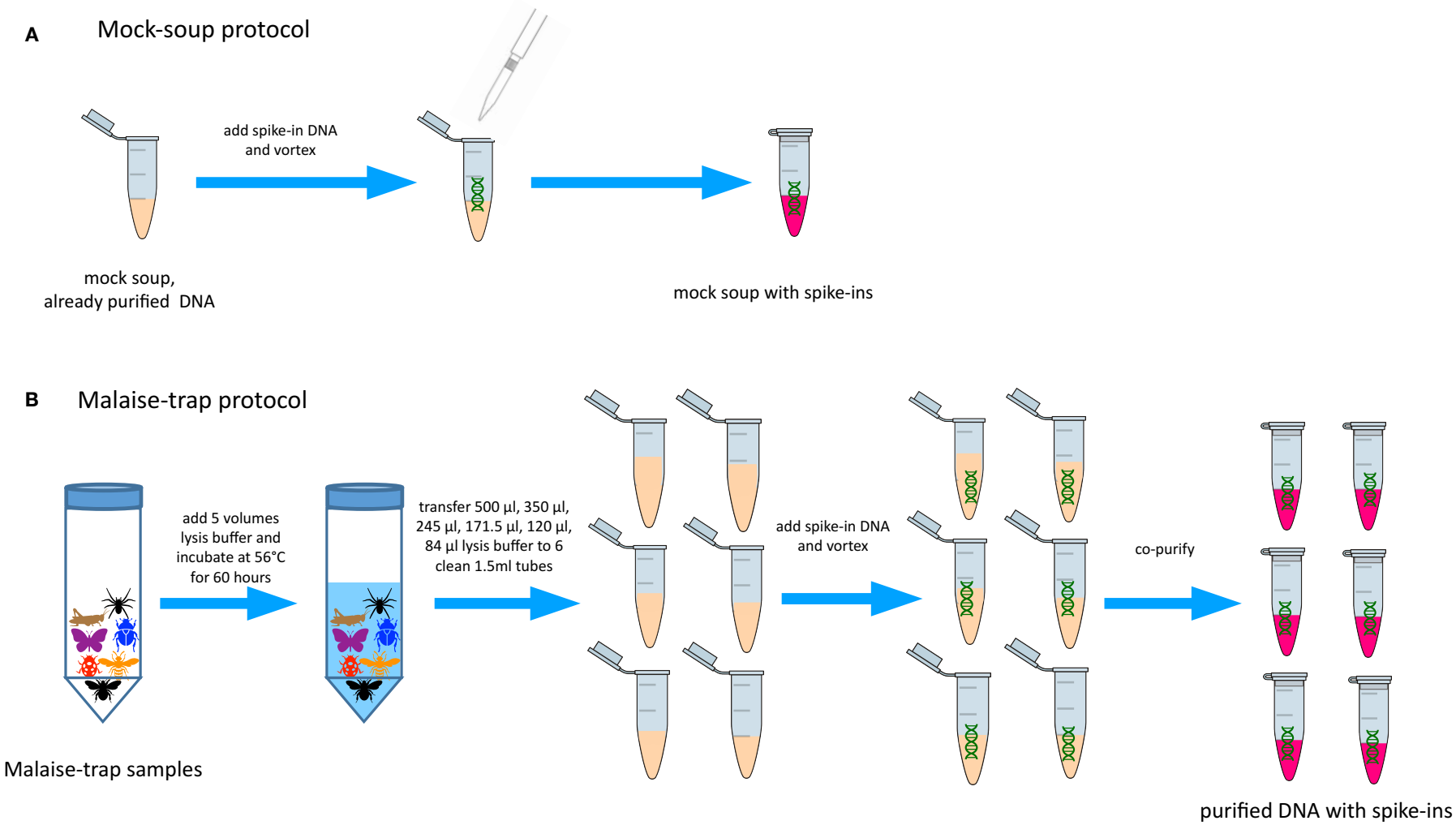


**Figure 5**. **DNA spike-in protocols**. A. Mock-soup protocol. Each mock soup was constructed by pooling purified DNA from individually extracted insects, after which a fixed aliquot of spike-in DNA was added to each pool. B. Malaise-trap-sample protocol. Each bulk sample of arthropods was non-destructively DNA-extracted by soaking in 5X volume of lysis buffer. From each of the 7 samples, 500 µl, 350 µl, 245 µl, 171.5 µl, 120 µl, and 84 µl lysis buffer was used to create 6 dilution soups, a fixed amount of spike-in DNA was added, and the mixture was co-purified. (**94 words**)

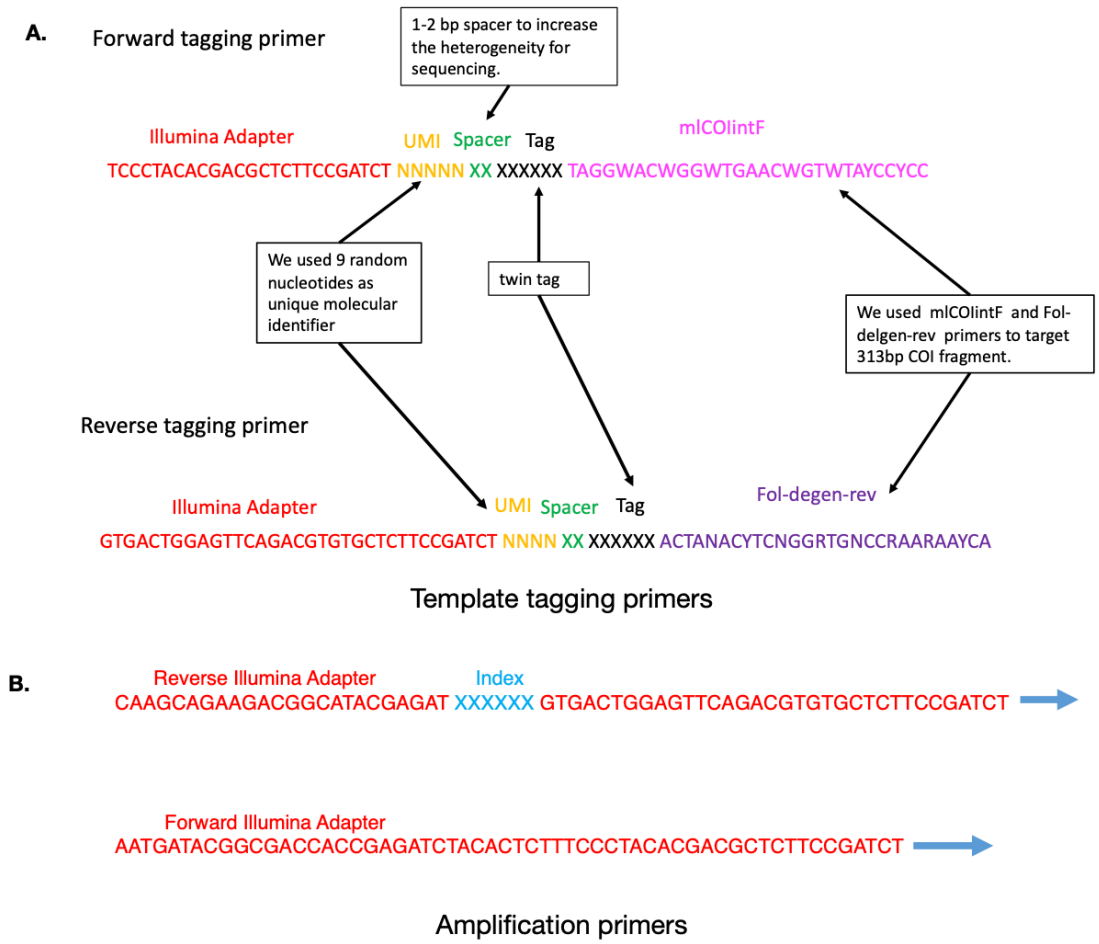


**Figure 6**. **Two-step PCR protocol**. A. In the first step, we amplified a 313 bp COI amplicon using the Leray-FolDegenRev primers. To both the forward and reverse primers, we added a 1-2 nucleotide heterogeneity spacer, the same 6-nucleotide sample tag (twin tags), a 9-random-nucleotide UMI (unique molecular identifier, split as 5 Ns on the forward and 4 Ns on the reverse), and a part of Illumina adapter sequence to anneal to the PCR primers in the second step. B. In the second step, we concatenated a library index sequence and the forward and reverse Illumina adapter sequences. Additional details on primer design (other than the UMI portion) can be found in Yang et al. (2021).(**115 words**)

356 *2.5 PCR and the Begum pipeline*. – The first PCR amplifies COI and concatenates
357 sample tags and UMIs and runs for only two cycles using KAPA 2G Robust HS PCR
358 Kit (Basel, Roche KAPA Biosystems). We used the mlCOIintF-FolDegenRev primer
359 pair (Yu et al. 2012, p. 2012; Leray et al. 2013), which amplifies a 313-bp fragment of
360 the COI barcode; and we followed the Begum protocol (Zepeda-Mendoza et al. 2016;
361 Yang et al. 2021), which is a wet-lab and bioinformatic pipeline that combines multiple
362 independent PCR replicates per sample, twin-tagging and false positive controls to
363 remove tag-jumping and reduce erroneous sequences. Twin-tagging means using the
364 same tag sequence on both the forward and reverse primers in a PCR. Tag jumps
365 almost always result in non-matching tag sequences, and these are identified and
366 removed in the Begum pipeline. We performed 3 PCR replicates per sample, which
367 means we used 3 different twin-tags to distinguish the 3 independent PCR replicates.
368 Begum removes erroneous sequences by filtering out the reads that appear in a low
369 number of PCR replicates (e.g. only one PCR) at a low number of copies per PCR (e.g.
370 only 2 copies), because true sequences are more likely to appear in multiple PCRs with
371 higher copy numbers per PCR. The 20 µl reaction mix included 4 µl Enhancer, 4 µl
372 Buffer A, 0.4 µl dNTP (10 mM), 0.8 µl per primer (10 mM), 0.08 µl KAPA 2G HotStart
373 DNA polymerase (Basel, Roche KAPA Biosystems), 5 µl template DNA and 5 µl water.
374 PCR conditions were initial denaturation at 95°C for 3 minutes, followed by two cycles
375 of denaturation at 95°C for 1 minute, annealing at 50°C for 90 seconds, and extension
376 at 72°C for 2 minutes. Then the products were purified with 14 µl of KAPA pure beads
377 (Roche KAPA Biosystems, Switzerland) to remove the primers and PCR reagents and
378 were eluted into 16 µl of water.

379 The second PCR amplifies the tagged templates for building the libraries that can be
380 sequenced directly on Illumina platform. The 50 µl reaction mix included 5 µl TAKARA
381 buffer, 4 µl dNTP (10 mM), 1.2 µl per primer (10 mM), 0.25 µl TAKARA Taq DNA
382 polymerase, 15 µl DNA product from the first PCR, and 23.35 µl water. PCR conditions
383 were initial denaturation at 95°C for 3 minutes, 5 cycles of denaturation at 95°C for 30
384 seconds, annealing at 59°C for 30 seconds (-1 °C per cycle), extension at 72°C for 30
385 seconds, followed by 25 cycles of denaturation at 95°C for 30 seconds, annealing at
386 55°C for 30 seconds, extension at 72°C for 30 seconds; a final extension at 72°C for 5
387 minutes, and cool down to 4°C.

388 From all second PCR products, 2 µl was roughly quantified on 2% agarose gel with
389 Image Lab 2.0 (Bio-Rad, USA). For each set of PCR reactions with the same index,
390 amplicons were mixed at equimolar ratios to make a pooled library. One PCR negative
391 control were set for each library. We sent our samples to Novogene (Tianjin, China) to

do PE250 sequencing on Illumina NovaSeq 6000, requiring a 0.8 GB raw data from each PCR reaction.

*2.6 Bioinformatic processing*. – AdapterRemoval 2.1.7 was used to remove any remaining adapters from the raw data (Schubert et al., 2016). Sickle 1.33 was used to trim away low-quality bases at the 3'ends. BFC V181 was used to denoise the reads (Li, 2015). Read merging was performed using Pandaseq 2.11 (Masella et al. 2012). Begum was used to demultiplex the reads by sample tag and to filter out erroneous reads (https://github.com/shyamsg/Begum, accessed 07 Sep 2021). We allowed 2-bp primer mismatches to the twin-tags while demultiplexing, and we filtered at a stringency of accepting only reads that appeared in at least two PCRs at a minimum copy number of 4 reads per PCR, with minimum length of 300 bp. This stringency minimized the false positive reads in the negative PCR control.

For mock-soup data, we need to compare the UMI and read numbers in each PCR set. However, Begum cannot recognize UMIs. Also because of our complicated primer structure, there is no software available for our data to count the UMIs per OTU in each PCR set. Thus, we wrote a custom bash script to process the mock-soup data from the Pandaseq output files, which include all the UMIs, tags, and primers. First, we used *Begum*-filtered sequences as a reference to filter reads for each PCR set, and put the UMI information on read headers. Then we carried out reference-based OTU clustering for each PCR set with Qiime 1.9.1 (`pick_otus.py -m uclust_ref -s 0.99`) (Caporaso et al. 2010; Edgar 2010), using the OTU representative sequences from barcoding Sanger sequencing as the reference, counted UMIs and reads for each OTU in each PCR set, and generated two OTU tables, separately with UMI and read numbers.

For the Malaise-trap data, we directly used the Begum pipeline. After Begum filtering, vsearch 2.14.1 (`--uchime_denovo`) (Rognes et al. 2016) was used to remove chimeras. Sumaclust 1.0.2 was used to cluster the sequences of Malaise-trap samples into 97% similarity OTUs. The python script tabulateSumaclust.py from the DAMe toolkit was used to generate the OTU table. Finally, we applied the R package LULU 0.1.0 with default parameters to merge oversplit OTUs (Frøslev et al. 2017). The OTU table and OTU representative sequences were used for downstream analysis.

*2.6 Statistical analyses*. – All statistical analyses were carried out in *R* 4.1.0 (R Core Team 2021), and we used the {lme4} 1.1-27 package (Bates et al. 2015) to fit linear mixed-effects models, using OTU, soup replicate, and PCR replicates as random factors. Model syntax is given in the legend of Figure 7. We used the {MuMIn} 1.43.17 package (CRAN.R-project.org/package=MuMIn, accessed 2 Jan 2022) to calculate the

428 variance explained by fixed effects only (marginal $R^2$). To carry out spike-in correction,
429 we first calculated a weighted mean from the added spike-ins (e.g. mean(Bombycidae
430 + Elateridae/2 + Mordellidae/4)), rescaled the new mean spike-in so that the smallest
431 value is equal to 1, and divided each row's OTU size and UMI number by the weighted,
432 scaled spike-in.

## 433 Results

434 *3.1 Bioinformatic processing of the Malaise-trap samples and the mock soups.* – Five
435 libraries yielded a total of 283,319,770 paired-end reads, of which 247,285,097 were
436 merged successfully in Pandaseq. After *Begum* sorting and demultiplexing, which
437 removed a large number of tag-jumped reads and some reads <300 bp length, we
438 retained 106,649,397 reads. After *Begum*'s erroneous-read filtering, we retained
439 76,289,802 reads, and after *de-novo* chimera removal, we retained 73,818,971 reads.
440 Sequences were clustered at 97% similarity into 1,188 OTUs, and LULU combined the
441 OTUs of the Malaise-trap samples into 435 OTUs. After removing the spike-in OTUs,
442 the seven Malaise-trap samples contained a total of 432 OTUs. All 52 OTUs of the 7
443 mock soups were recovered.

444 *3.2 Mock soups, COI copy number.* – Without spike-in correction, OTU size (numbers
445 of reads per OTU) predicts almost none of the within-species (across-sample) variation
446 in COI copy number ($R^2$ = 0.04, all values marginal $R^2$), but with spike-in correction,
447 OTU size predicts 42.0% of the variation (Figure 7 AB). As expected, UMI number by
448 itself does not predict input COI copy number ($R^2$ = 0.05), but with spike-in correction,
449 UMI number does predict COI copy number ($R^2$ = 0.42) (Figure 7 CD). Also as
450 expected, spike-in correction does not achieve across-species quantification, as shown
451 by the orders of magnitude variation in intercepts across the 52 OTUs. Note that this
452 experiment pooled DNA extracts with equalised concentrations of genomic DNA mass
453 per species, which suggests that PCR bias is the main source of species bias in this
454 dataset.

455 *3.4 Mock soup within-species abundance in input genomic DNA mass.* – Of course, our
456 goal is to estimate not COI copy number but specimen biomass. We thus tested how
457 well OTU size and UMI numbers predicted genomic DNA concentration. Non-spike-
458 corrected OTU size and UMI number both failed to predict input genomic DNA mass
459 ($R^2$ < 0.02 for both, Figure 8 AC), but spike-corrected OTU size and UMI number again
460 both successfully predicted input genomic DNA mass ($R^2$ = 0.52 and 0.53, Figure 8
461 BD).

*3.5 Malaise-trap within*-species *abundance recovery.* – Recall that each of the 7 selected Malaise-trap samples was serially diluted by 0.7X to create six soups per sample. Non-spike-corrected OTU size did not predict within-species variation in input genomic-DNA mass (p = 0.33) (Figure 9A), but spike-corrected OTU size again did predict within-species variation in input genomic-DNA mass ($R^2$ = 0.53) (Figure 9B).

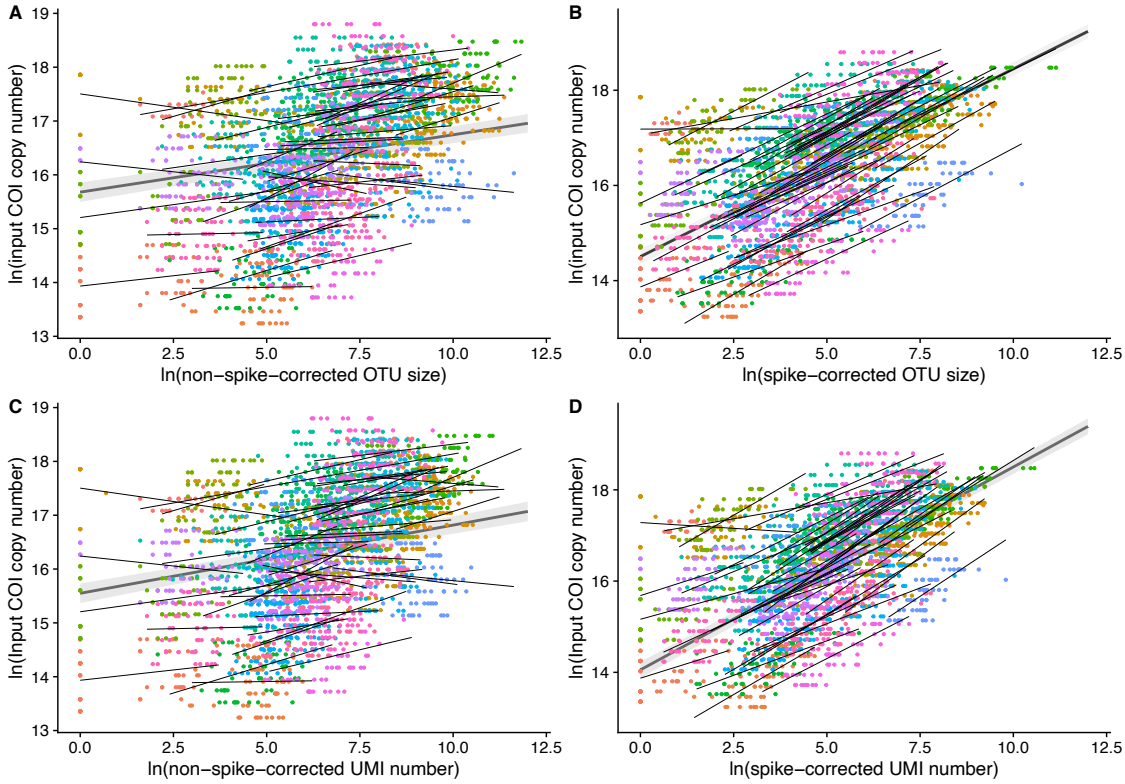


**Figure 7**. **Prediction of within-species variation in COI copy number in the mock-soup experiment**. For visualisation, all data points are shown (including all soup and PCR replicates), each thin line is fit to one of the OTUs across the seven serially diluted mock-soup samples, and the thick line represents the fitted model in which OTUs were treated as a random factor. **A**. Non-spike-corrected OTU size (number of reads per OTU per soup) poorly predicts within-species variation in input COI copy number (linear mixed-effects model, marginal $R^2$ = 0.04) (Bates et al. 2015). **B**. Spike-corrected OTU size successfully predicts within-species variation in input COI copy number (mixed-effects linear model, marginal $R^2$ = 0.42), but species bias remains, as can be seen in the orders-of-magnitude variation in intercepts (Figure 1). **C**. UMI number (per OTU per soup) poorly predicts within-species variation in input COI copy number (marginal $R^2$ = 0.05). **D**. Spike-corrected UMI number successfully predicts within-species variation in input COI copy number (marginal $R^2$ = 0.42), and again species bias remains, as shown by the different intercepts. Model syntax: `lme4::lmer(log.input_COI ~ log.OTUsize_or_UMINumber + (log.OTUsize_or_UMINumber | OTUID) + (1 |soupRep/pcrRep))`. (**169 words**)

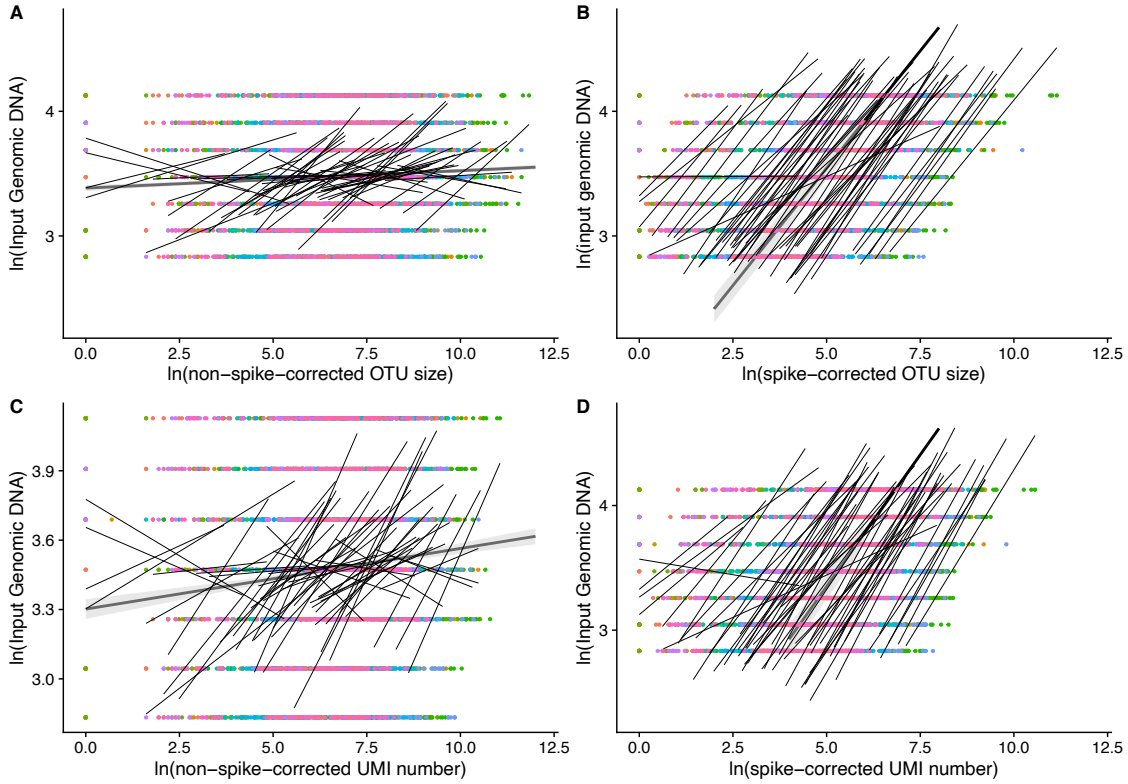


**Figure 8**. **Prediction of within-species variation in genomic DNA concentration in the mock-soup experiment**. For visualisation, all data points are shown (including all soup and PCR replicates), each thin line is fit to one of the OTUs across the seven serially diluted mock-soup samples, and the thick line represents the fitted model in which OTUs were treated as a random factor. **A**. Non-spike-corrected read number poorly predicts within-species variation in input genomic DNA concentration (linear mixed-effects model, marginal $R^2$ = 0.01). B. Spike-corrected read number successfully predicts within-species variation in input genomic DNA concentration (linear mixed-effects model, marginal $R^2$ = 0.52) despite species bias (Figure 1). C. UMI number poorly predicts within-species variation in input genomic DNA concentration (marginal $R^2$ = 0.02). D. Spike-corrected UMI number successfully predicts within-species variation in input genomic DNA concentration (marginal $R^2$ = 0.53) despite species biases. Model syntax: `lme4::lmer(log.input_gDNA ~ log.OTUsize_or_UMINumber + (log.OTUsize_or_UMINumber | OTUID) + (1 |soupRep/pcrRep))`. (**137 words**)

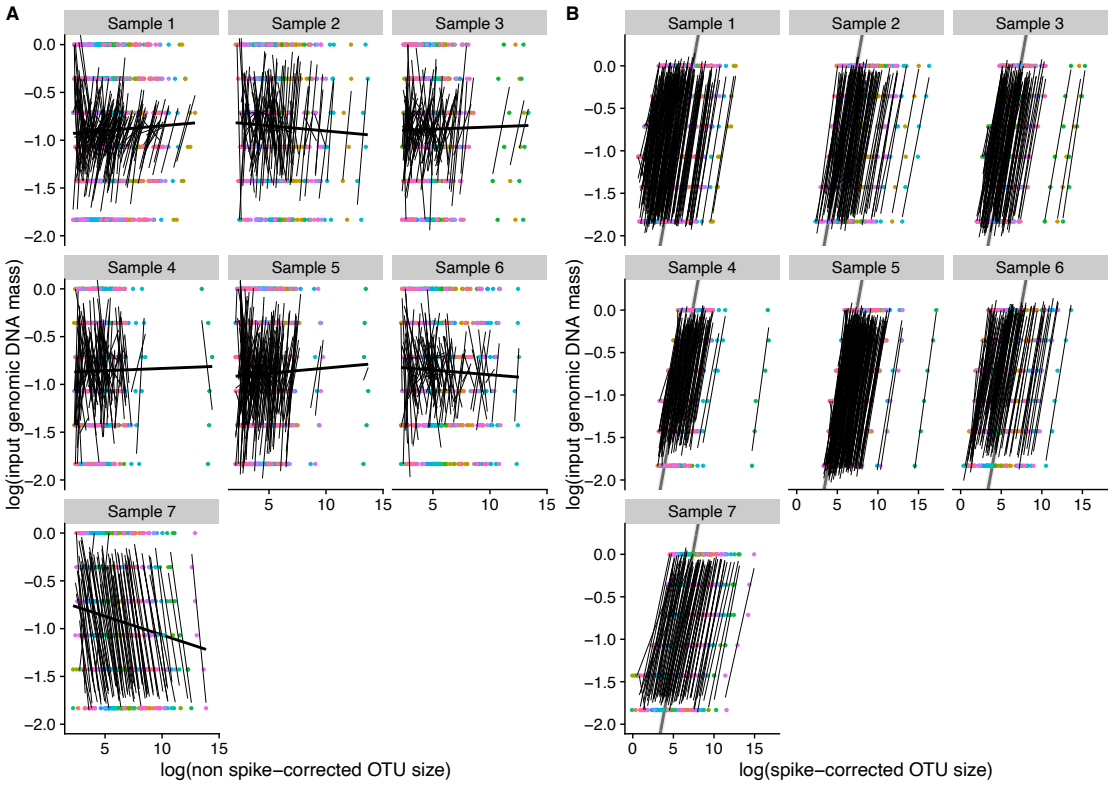


**Figure 9**. **Prediction of within-species variation in genomic DNA concentration in the Malaise-trap samples**. For visualisation, each thin line is fit to one of the OTUs within each of the seven serially diluted Malaise-trap samples, and the thick lines are fit to all points within a sample. There are 176, 113, 111, 104, 196, 110, and 82 OTUs in samples 1-7, respectively. **A**. Non-spike-corrected read number (OTU size) does not predict within-species variation in genomic DNA concentration ($p = 0.33$), and none of the random factors was retained. **B**. Spike-corrected read number successfully predicts within-species variation in genomic DNA concentration (marginal $R^2 = 0.53$) despite species bias, represented by the different intercepts. A similar protocol was followed in Ji et al. (2020), where it was called "FSL correction". **Full model syntax**: `lme4::lmer(log.input_gDNA ~ log.OTUsize + (log.OTUsize | sample/OTUID))`. (**136 words**)

## Discussion

We propose that there is a useful distinction to be made between *within*-species abundance change and *across*-species abundance differences (Figures 1, 2). Within-species abundance information is sufficient for inferring species interactions, modelling population dynamics and species distributions, detecting environmental state and change, and inferring false positives and negatives (Figure 3) . We experimentally show that spike-ins allow the recovery of within-species abundance change, which is expected since spike-ins remove pipeline noise.

522 In our first test, we serially diluted 52 OTUs into seven mock soups, and after spike-in
523 correction, we were able to recover within-species abundance change in both input
524 COI copy number (Figure 7) and input genomic DNA (Figure 8), the latter of which is
525 more closely correlated with organism biomass. In our second test, we serially diluted
526 each of seven Malaise-trap soups into six soups, and we were able to recover within-
527 species abundance change in input genomic DNA (Figure 9). Finally, our experimental
528 protocol included Unique Molecular Identifiers (UMIs), which required a laborious two-
529 step PCR protocol, but we found no additional quantification benefit over the spike-in.

530 In most cases, practitioners will need to add exogenous spike-ins to their samples
531 (Bates et al. 2015), but in the special but important case of host-associated
532 microbiomes, Lundberg et al. (2021) describe a two-step PCR method to use a single-
533 copy host gene as a built-in spike-in.

534 Statistical analysis of DNA-based datasets will also need to take into account the
535 potential ready availability of within-species abundance information. The most
536 straightforward method is to incorporate spike-in counts as an offset term in general
537 linear models. For species distribution modelling, there is a need for software packages
538 to utilise the information available in abundance data that ranges continuously from
539 [0,1], whereas to our knowledge, practitioners can effectively now only choose between
540 presence/absence and absolute-abundance data.

541 We conclude with the acknowledgment that relative species abundance remains the
542 more difficult abundance-estimation problem, given the many hidden sources of
543 species bias along metabarcoding and metagenomic pipelines (McLaren et al. 2019),
544 but promising solutions are now available in the {paramedic} *R* package (Williamson et
545 al. 2021) and in the metagenomic protocols of Lang et al. (2019) and Peel et al. (2019).
546 Note that even if species biases can be corrected by using one of these techniques, it
547 is still necessary to use a spike-in to correct for pipeline noise.

## 548 Data availability statement

549 R scripts and data for Figures 7, 9, and 9 are posted at
550 https://github.com/LoreMJ/quantitive_metabarcoding. All sequence data, reference
551 files, folder structure, output files and scripts (32.5 GB) on DataDryad.
552 (https://datadryad.org/stash/share/0rJ5Yy2PRIv5UpVrCS95Wf7pY0J2R_Hqic6DWyMe
553 aD8)

## Acknowledgments

We thank Sarah Bourlat and Nathan Geraldi for very helpful comments on the manuscript. D. W. Yu was supported by the Key Research Program of Frontier Sciences, CAS (QYZDY-SSW-SMC024), Supported by the Strategic Priority Research Program of Chinese Academy of Sciences, Grant No. XDA20050202, the University of East Anglia, the State Key Laboratory of Genetic Resources and Evolution (GREKF19-01, GREKF20-01, GREKF21-01) at the Kunming Institute of Zoology, the University of East Anglia, and the University of Chinese Academy of Sciences.

## References

Abrego, N., T. Roslin, T. Huotari, Y. Ji, N. M. Schmidt, J. Wang, D. W. Yu, et al. 2021. Accounting for species interactions is necessary for predicting how arctic arthropod communities respond to climate change. Ecography 44:885–896.

Amend, A. S., K. A. Seifert, and T. D. Bruns. 2010. Quantifying microbial communities with 454 pyrosequencing: does read abundance count? Molecular Ecology 19:5555–5565.

Bates, D., M. Mächler, B. Bolker, and S. Walker. 2015. Fitting Linear Mixed-Effects Models Using **lme4**. Journal of Statistical Software 67:1–48.

Bell, K. L., J. Fowler, K. S. Burgess, E. K. Dobbs, D. Gruenewald, B. Lawley, C. Morozumi, et al. 2017. Applying Pollen DNA Metabarcoding to the Study of Plant–Pollinator Interactions. Applications in Plant Sciences 5:1600124.

Brys, R., D. Halfmaerten, S. Neyrinck, Q. Mauvisseau, J. Auwerx, M. Sweet, and J. Mergeay. 2021. Reliable eDNA detection and quantification of the European weather loach ( *Misgurnus fossilis* ). Journal of Fish Biology 98:399–414.

Caporaso, J. G., J. Kuczynski, J. Stombaugh, K. Bittinger, F. D. Bushman, E. K. Costello, N. Fierer, et al. 2010. QIIME allows analysis of high-throughput community sequencing data. Nature Methods 7:335–336.

Carraro, L., E. Mächler, R. Wüthrich, and F. Altermatt. 2020. Environmental DNA allows upscaling spatial patterns of biodiversity in freshwater ecosystems. Nature Communications 11:3585.

Carraro, L., J. B. Stauffer, and F. Altermatt. 2021. How to design optimal eDNA sampling strategies for biomonitoring in river networks. Environmental DNA 3:157–172.

Creedy, T. J., H. Norman, C. Q. Tang, K. Qing Chin, C. Andujar, P. Arribas, R. S. O'Connor, et al. 2020. A validated workflow for rapid taxonomic assignment and

monitoring of a national fauna of bees (Apiformes) using high throughput DNA barcoding. Molecular Ecology Resources 20:40–53.

Deagle, B. E., L. J. Clarke, J. A. Kitchener, A. M. Polanowski, and A. T. Davidson. 2018. Genetic monitoring of open ocean biodiversity: An evaluation of DNA metabarcoding for processing continuous plankton recorder samples. Molecular Ecology Resources 18:391–406.

Deagle, B. E., A. C. Thomas, J. C. McInnes, L. J. Clarke, E. J. Vesterinen, E. L. Clare, T. R. Kartzinel, et al. 2019. Counting with DNA in metabarcoding studies: How should we convert sequence reads to dietary data? Molecular Ecology 28:391–406.

deWaard, J. R., V. Levesque-Beaudin, S. L. deWaard, N. V. Ivanova, J. T. A. McKeown, R. Miskie, S. Naik, et al. 2019. Expedited assessment of terrestrial arthropod diversity by coupling Malaise traps with DNA barcoding. Genome 62:85–95.

Doi, H., K. Fukaya, S. Oka, K. Sato, M. Kondoh, and M. Miya. 2019. Evaluation of detection probabilities at the water-filtering and initial PCR steps in environmental DNA metabarcoding using a multispecies site occupancy model. Scientific Reports 9:3581.

Dorazio, R. M., and R. A. Erickson. 2018. ednaoccupancy : An R package for multiscale occupancy modelling of environmental DNA data. Molecular Ecology Resources 18:368–380.

Edgar, R. C. 2010. Search and clustering orders of magnitude faster than BLAST. Bioinformatics 26:2460–2461.

Elbrecht, V., and F. Leese. 2015. Can DNA-Based Ecosystem Assessments Quantify Species Abundance? Testing Primer Bias and Biomass—Sequence Relationships with an Innovative Metabarcoding Protocol. PLOS ONE 10:e0130324.

Erickson, R. A. 2019. Sampling Designs for Landscape-level eDNA Monitoring Programs. Integr Environ Assess Manag 12.

Frøslev, T. G., R. Kjøller, H. H. Bruun, R. Ejrnæs, A. K. Brunbjerg, C. Pietroni, and A. J. Hansen. 2017. Algorithm for post-clustering curation of DNA amplicon data yields reliable biodiversity estimates. Nature Communications 8:1188.

Fukaya, K., H. Murakami, S. Yoon, K. Minami, Y. Osada, S. Yamamoto, R. Masuda, et al. 2021. Estimating fish population abundance by integrating quantitative data on environmental DNA and hydrodynamic modelling. Molecular Ecology 30:3057–3067.

Garrido-Sanz, L., M. À. Senar, and J. Piñol. 2021. Relative species abundance estimation in artificial mixtures of insects using mito-metagenomics and a correction

620 factor for the mitochondrial DNA copy number. Molecular Ecology Resources 1755–
621 0998.13464.

622 Griffin, J. E., E. Matechou, A. S. Buxton, D. Bormpoudakis, and R. A. Griffiths. 2020.
623 Modelling environmental DNA data; Bayesian variable selection accounting for false
624 positive and false negative errors. Journal of the Royal Statistical Society: Series C
625 (Applied Statistics) 69:377–392.

626 Harrison, J. G., W. John Calder, B. Shuman, and C. Alex Buerkle. 2021. The quest for
627 absolute abundance: The use of internal standards for DNA-based community ecology.
628 Molecular Ecology Resources 21:30–43.

629 Hebert, P. D. N., T. W. A. Braukmann, S. W. J. Prosser, S. Ratnasingham, J. R.
630 deWaard, N. V. Ivanova, D. H. Janzen, et al. 2018. A Sequel to Sanger: amplicon
631 sequencing that scales. BMC Genomics 19:219.

632 Hindson, B. J., K. D. Ness, D. A. Masquelier, P. Belgrader, N. J. Heredia, A. J.
633 Makarewicz, I. J. Bright, et al. 2011. High-Throughput Droplet Digital PCR System for
634 Absolute Quantitation of DNA Copy Number. Analytical Chemistry 83:8604–8610.

635 Hoshino, T., and F. Inagaki. 2017. Application of Stochastic Labeling with Random-
636 Sequence Barcodes for Simultaneous Quantification and Sequencing of Environmental
637 16S rRNA Genes. PLOS ONE 12:e0169431.

638 Hoshino, T., R. Nakao, H. Doi, and T. Minamoto. 2021. Simultaneous absolute
639 quantification and sequencing of fish environmental DNA in a mesocosm by
640 quantitative sequencing technique. Scientific Reports 11:4372.

641 Ji, Y., T. Huotari, T. Roslin, N. M. Schmidt, J. Wang, D. W. Yu, and O. Ovaskainen.
642 2020. SPIKEPIPE: A metagenomic pipeline for the accurate quantification of eukaryotic
643 species occurrences and intraspecific abundance change using DNA barcodes or
644 mitogenomes. Molecular Ecology Resources 20:256–267.

645 Krehenwinkel, H., M. Wolf, J. Y. Lim, A. J. Rominger, W. B. Simison, and R. G.
646 Gillespie. 2017. Estimating and mitigating amplification bias in qualitative and
647 quantitative arthropod metabarcoding. Scientific Reports.

648 Lang, D., M. Tang, J. Hu, and X. Zhou. 2019. Genome-skimming provides accurate
649 quantification for pollen mixtures. Molecular Ecology Resources 19:1433–1446.

650 Leray, M., J. Y. Yang, C. P. Meyer, S. C. Mills, N. Agudelo, V. Ranwez, J. T. Boehm, et
651 al. 2013. A new versatile primer set targeting a short fragment of the mitochondrial COI
652 region for metabarcoding metazoan diversity: application for characterizing coral reef
653 fish gut contents. Frontiers in Zoology 10:34.

654 Levi, T., J. M. Allen, D. Bell, J. Joyce, J. R. Russell, D. A. Tallmon, S. C. Vulstek, et al.
655 2019. Environmental DNA for the enumeration and management of Pacific salmon.
656 Molecular Ecology Resources 19:597–608.

657 Li, H. 2015. BFC: correcting Illumina sequencing errors. Bioinformatics 31:2885–2887.

658 Lundberg, D. S., P. P. N. Ayutthaya, A. Strauß, G. Shirsekar, W.-S. Lo, T. Lahaye, and
659 D. Weigel. 2021. Host-associated microbe PCR (hamPCR) enables convenient
660 measurement of both microbial load and community composition. eLife 10:e66186.

661 Lundberg, D. S., S. Yourstone, P. Mieczkowski, C. D. Jones, and J. L. Dangl. 2013.
662 Practical innovations for high-throughput amplicon sequencing. Nature Methods
663 10:999–1002.

664 Lyet, A., L. Pellissier, A. Valentini, T. Dejean, A. Hehmeyer, and R. Naidoo. 2021.
665 eDNA sampled from stream networks correlates with camera trap detection rates of
666 terrestrial mammals. Scientific Reports 11:11362.

667 Masella, A. P., A. K. Bartram, J. M. Truszkowski, D. G. Brown, and J. D. Neufeld. 2012.
668 PANDAseq: paired-end assembler for illumina sequences. BMC Bioinformatics 13:31.

669 McLaren, M. R., A. D. Willis, and B. J. Callahan. 2019. Consistent and correctable bias
670 in metagenomic sequencing experiments. eLife 8:e46923.

671 Meier, R., W. Wong, A. Srivathsan, and M. Foo. 2016. $1 DNA barcodes for
672 reconstructing complex phenomes and finding rare species in specimen-rich samples.
673 Cladistics 32:100–110.

674 Nielsen, M., M. T. P. Gilbert, T. Pape, and K. Bohmann. 2019. A simplified DNA
675 extraction protocol for unsorted bulk arthropod samples that maintains exoskeletal
676 integrity. Environmental DNA 1:144–154.

677 Pauvert, C., M. Buée, V. Laval, V. Edel-Hermann, L. Fauchery, A. Gautier, I. Lesur, et
678 al. 2019. Bioinformatics matters: The accuracy of plant and soil fungal community data
679 is highly dependent on the metabarcoding pipeline. Fungal Ecology 41:23–33.

680 Peel, N., L. V. Dicks, M. D. Clark, D. Heavens, L. Percival-Alwyn, C. Cooper, R. G.
681 Davies, et al. 2019. Semi-quantitative characterisation of mixed pollen samples using
682 MinION sequencing and Reverse Metagenomics (RevMet). Methods in Ecology and
683 Evolution 10:1690–1701.

684 Piñol, J., G. Mir, P. Gomez-Polo, and N. Agustí. 2015. Universal and blocking primer
685 mismatches limit the use of high-throughput DNA sequencing for the quantitative
686 metabarcoding of arthropods. Molecular Ecology Resources 15:819–830.

Piñol, J., M. A. Senar, and W. O. C. Symondson. 2019. The choice of universal primers and the characteristics of the species mixture determine when DNA metabarcoding can be quantitative. Molecular Ecology 28:407–419.

Pochardt, M., J. M. Allen, T. Hart, S. D. L. Miller, D. W. Yu, and T. Levi. 2020. Environmental DNA facilitates accurate, inexpensive, and multiyear population estimates of millions of anadromous fish. Molecular Ecology Resources 20:457–467.

R Core Team. 2021. R: A language and environment for statistical computing. R Foundation for Statistical Computing, Vienna, Austria.

Ratnasingham, S. 2019. mBRAVE: The Multiplex Barcode Research And Visualization Environment. Biodiversity Information Science and Standards 3:e37986.

Rognes, T., T. Flouri, B. Nichols, C. Quince, and F. Mahé. 2016. VSEARCH: a versatile open source tool for metagenomics. PeerJ 4:e2584.

Rojahn, J., L. Pearce, D. M. Gleeson, R. P. Duncan, D. M. Gilligan, and J. Bylemans. 2021. The value of quantitative environmental DNA analyses for the management of invasive and endangered native fish. Freshwater Biology fwb.13779.

Schenk, J., S. Geisen, N. Kleinboelting, and W. Traunspurger. 2019. Metabarcoding data allow for reliable biomass estimates in the most abundant animals on earth. Metabarcoding and Metagenomics 3:e46704.

Schubert, M., S. Lindgreen, and L. Orlando. 2016. AdapterRemoval v2: rapid adapter trimming, identification, and read merging. BMC Research Notes 9:88.

Shelton, A. O., J. L. O'Donnell, J. F. Samhouri, N. Lowell, G. D. Williams, and R. P. Kelly. 2016. A framework for inferring biological communities from environmental DNA. Ecological Applications 26:1645–1659.

Smets, W., J. W. Leff, M. A. Bradford, R. L. McCulley, S. Lebeer, and N. Fierer. 2016. A method for simultaneous measurement of soil bacterial abundances and community composition via 16S rRNA gene sequencing. Soil Biology and Biochemistry 96:145–151.

Srivathsan, A., L. Lee, K. Katoh, E. Hartop, S. N. Kutty, J. Wong, D. Yeo, et al. 2021. MinION barcodes: biodiversity discovery and identification by everyone, for everyone. BioRXiv doi:10.1101/2021.03.09.434692.

Stauffer, S., M. Jucker, T. Keggin, V. Marques, M. Andrello, S. Bessudo, M.-C. Cheutin, et al. 2021. How many replicates to accurately estimate fish biodiversity using environmental DNA on coral reefs? BioRxiv doi:10.1101/2021.05.26.445742.

Steinke, D., T. W. Braukmann, L. Manerus, A. Woodhouse, and V. Elbrecht. 2021. Effects of Malaise trap spacing on species richness and composition of terrestrial arthropod bulk samples. Metabarcoding and Metagenomics 5:e59201.

Tang, M., C. J. Hardman, Y. Ji, G. Meng, S. Liu, M. Tan, S. Yang, et al. 2015. High-throughput monitoring of wild bee diversity and abundance via mitogenomics. Methods in Ecology and Evolution 6:1034–1043.

Thalinger, B., A. Rieder, A. Teuffenbach, Y. Pütz, T. Schwerte, J. Wanzenböck, and M. Traugott. 2021. The Effect of Activity, Energy Use, and Species Identity on Environmental DNA Shedding of Freshwater Fish. Frontiers in Ecology and Evolution 9:623718.

Thomas, A. C., B. E. Deagle, J. P. Eveson, C. H. Harsch, and A. W. Trites. 2016. Quantitative DNA metabarcoding: improved estimates of species proportional biomass using correction factors derived from control material. Molecular Ecology Resources 16:714–726.

Tkacz, A., M. Hortala, and P. S. Poole. 2018. Absolute quantitation of microbiota abundance in environmental samples. Microbiome 6:110.

Verkuil, Y. I., M. Nicolaus, R. Ubels, M. M. Dietz, J. M. Samplonius, A. Galema, K. Kiekebos, et al. 2020. DNA metabarcoding successfully quantifies relative abundances of arthropod taxa in songbird diets: a validation study using camera-recorded diets. BioRxiv doi:10.1101/2020.11.26.399535.

Wang, Y., U. Naumann, S. T. Wright, and D. I. Warton. 2012. mvabund - an R package for model-based analysis of multivariate abundance data. Methods in Ecology and Evolution 3:471–474.

Williamson, B. D., J. P. Hughes, and A. D. Willis. 2021. A multiview model for relative and absolute microbial abundances. Biometrics doi:10.1111/biom.13503.

Wührl, L., C. Pylatiuk, M. Giersch, F. Lapp, T. von Rintelen, M. Balke, S. Schmidt, et al. 2021. DiversityScanner: Robotic discovery of small invertebrates with machine learning methods. BioRxiv doi:10.1101/2021.05.17.444523.

Yang, C., K. Bohmann, X. Wang, W. Cai, N. Wales, Z. Ding, S. Gopalakrishnan, et al. 2021. Biodiversity Soup II: A bulk-sample metabarcoding pipeline emphasizing error reduction. Methods in Ecology and Evolution 12:1252–1264.

Yates, M. C., M. E. Cristescu, and A. M. Derry. 2021*a*. Integrating physiology and environmental dynamics to operationalize environmental DNA (eDNA) as a means to monitor freshwater macro-organism abundance. Molecular Ecology mec.16202.

754 Yates, M. C., D. M. Glaser, J. R. Post, M. E. Cristescu, D. J. Fraser, and A. M. Derry.
755 2021*b*. The relationship between eDNA particle concentration and organism
756 abundance in nature is strengthened by allometric scaling. Molecular Ecology
757 30:3068–3082.

758 Yu, D. W., Y. Ji, B. C. Emerson, X. Wang, C. Ye, C. Yang, and Z. Ding. 2012.
759 Biodiversity soup: metabarcoding of arthropods for rapid biodiversity assessment and
760 biomonitoring. Methods in Ecology and Evolution 3:613–623.

761 Zepeda-Mendoza, M. L., K. Bohmann, A. Carmona Baez, and M. T. P. Gilbert. 2016.
762 DAMe: a toolkit for the initial processing of datasets with PCR replicates of double-
763 tagged amplicons for DNA metabarcoding analyses. BMC Research Notes 9:255.

764 Zhou, X., Y. Li, S. Liu, Q. Yang, X. Su, L. Zhou, M. Tang, et al. 2013. Ultra-deep
765 sequencing enables high-fidelity recovery of biodiversity for bulk arthropod samples
766 without PCR amplification. GigaScience 2:4.

767

# Supplementary Information: Unabridged Methods

*1 Mock soup construction*

*1.1 Input species*. – We used Malaise traps to collect 286 arthropods in Kunming, China (25°8'23" N, 102°44'17" E). DNA was extracted from each individual using the DNeasy Blood & Tissue Kit (Qiagen GmbH, Germany). Mean genomic DNA per species concentration was quantified from three replicates using PicoGreen fluorescent dye. We DNA-barcoded the individuals using the Folmer primer pair LCO1490 5'-GGTCAACAAATCATAAAGATATTGG -3', and HC02198 (5'-TAAACTTCAGGGTGACCAAAAAATCA -3') (Folmer et.al 1994) , with PCR parameters of initial denaturation at 95°C for 3 minutes, followed by 34 cycles of denaturation at 94°C for 30 seconds, annealing at 50°C for 30 seconds and extension at 72°C for 1 minute, a final extension at 72° C for 5 minutes, and a cooldown to 4°C. After the 658-bp COI sequences were cut to 313 bp based on our metabarcoding primers (see below), 286 arthropods were clustered into 168 OTUs at 97% similarity. To create mock soups, we selected 52 individuals with genomic DNA >20 ng/µl, representing 52 OTUs.

*1.2 OTU quantification*. – We quantified COI concentrations of the 52 OTUs using the mean of three qPCRs with the *Leray-FolDegenRev* primer pair (Yu et al. 2012; Leray et al. 2013). First, to create a standard DNA curve, we used a purified and sequenced COI amplicon (Lepidoptera Bombycidae *Bombyx mori*) and quantified its concentration with a Qubit, from which we calculated COI copy number from the COI concentration (ng/µl), molar mass (233530.15 g/mol), and the Avogadro constant.

$$COI\ copy\ number\ = \frac{COI\ concentration \times 10^{-9}}{molar\ mass} \times 6.02 \times 10^{23} \quad \text{(Eq. 1)}$$

This was 0.5X serially diluted into six concentration levels, as follows:

1. Start by diluting the above PCR amplicon to 100x by transferring 5 µl of amplicon to 495 µl of Ultragrade water. Vortex for 20 sec. Label as Tube 1.
2. Label 5 tubes from 2 to 6 and add 250 µl of water into each tube.
3. Transfer 250 µl from Tube 1 to Tube 2, and vortex for 20 sec.
4. Transfer 250 µl from Tube 2 to Tube 3, and vortex for 20 sec.
5. Continue the dilution series to Tube 6.
6. Use Tubes 1-6 as the standard DNA gradient for qPCR.

For each of the 52 OTUs, we used qPCR to quantify COI concentration (copy/µl). qPCRs were performed in a total volume of 20 µl with 10 µl of TAKARA SYBR premix Ex Taq (TaKaRa Biosystems, Dalian, China), 0.4 µl of Rox, 0.8 µl each of 10 µM of Leray and FolDegenRev primers (synthesized by Invitrogen, Shanghai, China), 2 µl of template DNA, and 6 µl of PCR-grade water. The qPCR conditions were 30 sec of initial denaturation at 95°C, followed by 35 cycles of denaturation at 95°C for 10 sec, 30 sec of annealing at 50°C, and 30 sec of extension at 72°C. Each OTU was quantified twice.

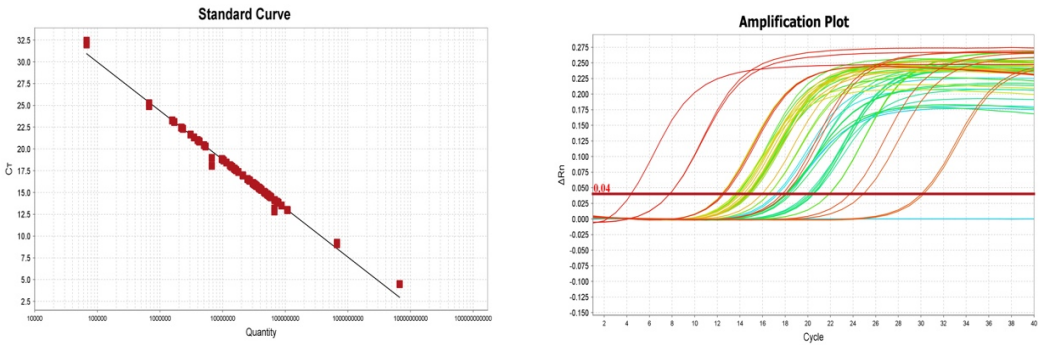


Figure **qPCR**. Left. qPCR standard curve (CT ~ input-COI concentration). Right. qPCR amplification curves, with the 12 (= 2 replicates x 6 concentrations) red lines representing the standard-DNA curves. The other colors represent the 52 OTUs, each amplified twice. All OTU curves lie within the bounds of the standard-DNA curves, allowing interpolation of absolute COI concentrations.

*1.3 Creation of mock soups*. – Each mock soup was constructed with equal masses of purified genomic DNA from 52 OTUs. Input genomic DNA masses of each OTU from soup 1 to soup 7 decreased by 0.8X to create seven mock soups of differing absolute abundances. The individual-OTU genomic DNA masses for the seven mock soups were 61, 48.8, 39, 31.2, 25, 20, and 16 ng and were independently added to the mock soups. Each of the seven soups was made in triplicate ($n_{tot}$ = 21).

*2 Preparation of Malaise-trap samples*

2.1 *Malaise trap sampling*. – 244 Malaise-trap samples from 96 sites, using 99.9% ethanol as the trapping liquid, were collected in and near a 384 $km^2$ forested landscape containing the H.J. Andrews Experimental Forest (44.2° N, 122.2° W), Oregon, United States in July 2018. Traps were left for 7 non-rainy days. To equalize biomass across individuals, we only kept the heads of large individuals (body lengths >2 cm) and then transferred the samples to fresh 99.9% ethanol to store at room temperature until extraction.

827 2.2 *DNA extraction*. – The samples were air dried individually on filter papers for less
828 than an hour and then transferred to 50 ml tubes or 5 ml tubes according to sample
829 volume. The samples were then weighed. DNA was non-destructively extracted by
830 soaking the samples in lysis buffer, using the protocol from Ji et al. (2020) and Nielsen
831 et al. (2019). In short, we added lysis buffer to each sample at a 5 ml:1 mg volume:air-
832 dried-mass ratio and incubated the samples in an incubator at 56°C, shaking for 60 hrs.
833 The recipe to make 50 ml of lysis buffer is 2 ml of 1M Tris-HCl buffer (PH 8.0), 1 ml of
834 5M sodium chloride, 10 ml of 10% Sodium Dodecyl Sulfate, 150 µl of 1M calcium
835 chloride, 34.225 ml of PCR-grade water, 2 ml of 1M Dithiothreitol, and 625 µl of
836 Proteinase K solution (20 mg/ml). After extraction, visual checks confirmed that the
837 extracted insects largely retained their body shapes, although they became darker.
838 Note that non-destructive DNA extraction increases the effects of species biases since
839 species with hard exoskeletons likely release less tissue.

840 For this study, we selected seven samples spread over the study area. After
841 completion of lysis, we serially diluted the 7 samples by using 0.7X lysis buffer volume
842 (500 µl, 350 µl, 245 µl, 171.5 µl, 120 µl and 84 µl) to create six soups per sample ($n_{tot}$ =
843 42). We used QIAquick PCR purification kit (Qiagen GmbH, Germany) by following the
844 manufacturer instructions to purify lysis buffer on one spin column per soup.

845 *3 Adding spike-in DNA*

846 *3.1 Spike-in DNA*. – For our spike-ins, we used three insect species from China, none
847 of which is expected to appear in the Oregon Malaise-trap samples (Table S1). An
848 alternative is to use one or more synthetic, random DNA sequences (Tkacz et al.
849 2018). Each of our three spike-ins is represented by a 658-bp COI fragment (Table 1)
850 with primer binding sites that match the Folmer primers HCO2198 and LCO1490. For
851 long-term storage, we inserted the COI fragments as plasmids into monoclonal
852 bacteria. Plasmids were extracted using TIANprep Mini Plasmid Kit (Beijing, China)
853 following manufacturer's instructions.

854 qPCR was used to quantify the three spike-in DNA COI concentrations (ng/µl) using
855 TAKARA SYBR Premix Ex Taq (TaKaRa Bio, Japan). COI copy numbers of the three
856 spike-in DNA were calculated using equation 1.

857 In our plan, we will mix the three spike-ins in a ratio of 1:2:4
858 (Bombycidae:Elateridae:Mordellidae), to check for error and degradation; the reads
859 from the three spike-ins should be found in the ratio of 1:2:4, but if, for instance, one of

860 the spike-ins is not at the correct ratio with the other two, we can omit that species'
861 reads and recalculate the spike-in correction.

| species | full COI barcode sequences |
|---|---|
| Lepidoptera Bombycidae<br>*Bombyx mori* | AACATTATATTTTATTTTTGGTATTTGATCAGGAATAATTGGAACATCTTTAAGACTT<br>TTAATTCGAGCTGAATTAGGAAATCCAGGATCATTAATTGGAGATGATCAAATTTAT<br>AATACTATTGTAACAGCACATGCTTTTATTATAATTTTTTTTATAGTTATACCTATTAT<br>AATTGGAGGATTTGGAAATTGATTAGTTCCTCTTATACTAGGAGCACCAGATATAG<br>CATTCCCACGAATAAATAATATAAGATTTTGACTCCTACCCCCCTCCCTTATATTAT<br>TAATTTCAAGAAGAATTGTAGAAAATGGTGCAGGAACAGGATGAACAGTTTACCCC<br>CCACTTTCATCTAATATCGCACATAGAGGAAGATCCGTAGATCTTGCTATTTTTTCA<br>CTACATTTAGCAGGTATTTCATCAATTATAGGAGCAATTAATTTTATTACAACAATA<br>ATTAATATACGATTAAATAATATATCATTTGATCAATTACCCTTATTTGTATGAGCTG<br>TAGGGATTACAGCATTTTTATTATTATTATCACTACCTGTTTTAGCTGGAGCTATTA<br>CAATATTATTAACAGATCGAAACTTAAATACATCATTTTTTGATCCTGCTGGAGGAG<br>GAGACCCAATTTTATATCAACATTTATTT |
| Coleoptera Elateridae sp. | AACTCTATACTTCATTTTTGGTGCCTGATCAGGAATACTAGGAACATCCTTAAGATT<br>ACTAATCCGTGCAGAACTAGGAAACCCAGGGGCACTAATTGGAAATGACCAAATT<br>TACAATGTTGTTGTTACAGCCCATGCATTTATCATAATTTTCTTCATAGTTATACCTA<br>TCATAATTGGTGGATTCGGAAATTGGTTAGTCCCTTTAATGCTAGGGGCACCAGAT<br>ATAGCTTTCCCTCGAATAAATAACATAAGATTCTGACTTCTCCCACCTTCCCTCAG<br>ATTGCTTTTAATGAGTAGAATTGTTGAAAGAGGGGCTGGGACTGGATGAACTGTTT<br>ATCCACCTTTAGCAGCAAACATTGCCCACAGAGGATCTTCTGTAGATTTAGCTATT<br>TTTAGTCTCCATTTAGCAGGAATTTCATCAATTTTAGGCGCTGTAAATTTCATCTCA<br>ACTGTAATCAACATGCGATCCACAGGGATAACTTTTGACCGTATACCTCTATTTGT<br>TTGAGCAGTTGCCATTACAGCCCTCCTTCTTCTTTTGTCTCTTCCTGTCCTTGCAG<br>GAGCAATTACAATACTTTTAACAGACCGAAACTTAAACACCTCATTTTTTGACCCAG<br>CAGGAGGAGGGGACCCAATTCTTTACCAACACTTATTC |
| Coleoptera Mordellidae sp. | AACACTTTATTTTATTTTTGGGGCCTGGGCAGGCATATTGGGAACGTCTCTAAGAT<br>TATTAATTCGATCAGAATTAGGAACCCCAGGAACTCTGATTGGAGATGACCAAATT<br>TACAACGTAATTGTTACAGCTCATGCTTTCGTAATAATTTTTTTTATAGTTATGCCT<br>GTAATAGTAGGGGGATTCGGCAATTGATTAGTTCCTCTTATATTAGGAGCACCTGA<br>CATAGCATTCCCCCGACTCAATAATATAAGATTTTGATTATTGCCCCCCTCTCTTTC<br>TTTATTACTAATGAGAAGATTAGTCGAAAACGGTGCCGGAACAGGATGTACAGTAT<br>ACCCCCCTTTATCTGCAAATCTAGCCCACGGAGGAGCTTCTGTAGATCTAGCCAT<br>CTTCAGTCTACATCTAGCAGGAATCTCATCAATTTTAGGAGCAATTAATTTTATCTC<br>AACTATACTTAATATACGTCCAATAGGAATAACATTAGATCGACTACCTTTATTTGT<br>TTGAGCTATTGTAATTACAGCAGTCCTATTGCTTTTATCCCTACCCGTTCTCGCAG<br>GGGCTATTACCATATTATTAACAGATCGAAATCTAAATACCTCATTTTTTGACCCTG<br>CAGGAGGGGGAGATCCTATTCTTTATCAACACTTATTC |

862 Table S1. DNA-barcode sequences of the three spike-in species.

| species | COI concentration (ng/µl) | COI copy number (copy/µl) |
|---|---|---|
| Lepidoptera Bombycidae<br>*Bombyx mori* | 0.0002 | $5.17 * 10^5$ |
| Coleoptera Elateridae sp. | 0.3914 | $1.02 * 10^9$ |
| Coleoptera Mordellidae sp. | 0.05807 | $1.51 * 10^8$ |

863 Table S2. COI concentrations of the three spike-in species

*3.2 Adding spike-in to the mock soups*. – Adding too much spike-in wastes sequencing data, while adding too little risks loss of abundance information in at least some samples when the number of spike-in reads is too low to use as a reliable correction factor. Thus, we quantified the COI copy numbers of the mock soups by qPCR and chose a volume so that spike-in reads should make up 1% of the total number of COI copies in the lowest-concentration mock soups, balancing efficiency with reliability.

Because we mixed 52 individual OTUs to create the mock soups, we can sum the input COI copy numbers of all 52 OTUs to calculate the COI copy number of the lowest-concentration mock soup ($5.25 * 10^8$ copies). We used 1% of this number to calculate the mass of total spike-in to add to all 21 soups ($5.25 * 10^6$ copies). To mix spike-ins DNA conveniently, the Elateridae spike-in was diluted 1000-fold to $1.02 * 10^6$ copies and the Mordellidae spike-in was diluted 100-fold to $1.51 * 10^6$ copies before mixing. Then we added 1.45 µl of *Bombyx* spike-in ($1.45 * 5.17 *10^5 = 0.75 * 10^6$), 1.5 µl of diluted Elateridae ($1.5 * 1.02 * 10^6 = 1.5 * 10^6$) and 2 µl of diluted Mordellidae ($2 * 1.51 * 10^6 = 3 * 10^6$) to each soup.

The sum of the three spike-ins was thus: $(0.75+1.5+3)\times 10^6 = 5.25\times 10^6$, and their ratio was: $0.75 \times 10^6 :1.5 \times10^6 :3 \times 10^6=1:2:4$.

Spike-in DNA was added directly to the mock soups' DNA since they were already purified (Figure 5).

*3.3 Adding spike-in to the Malaise-trap samples*. – From the 244 Malaise-trap samples, we first extracted 17 Malaise-trap samples without adding spike-ins, and then in order to decide how much spike-in should be added, we used qPCR to quantify the COI concentrations of these 17 Malaise-trap samples, using the same protocol that we used for the mock-soup OTUs. The mean COI concentration per sample was 0.006 ng/µl, for each of which we added 200 µl volume. Mean COI mass per aliquot was thus 1.2 ng (0.006 ng/µl x 200 µl), and 1% is 0.012 ng.

Because the Bombycid DNA spike-in had degraded after we arrived in University of Oregon where we extracted DNA from the Malaise-trap samples, we used only the other two spike-in species for the Malaise trap samples, at a ratio of 1:9 (Mordellidae:Elateridae). Mordellidae and Elateridae were re-quantified by qPCR and were diluted 100-fold. We added 2.7 µl of diluted Elateridae (2.7 µl * 0.004 ng/µl = 0.0108 ng) and 2 µl of diluted Mordellidae (2 µl * 0.0006 ng/µl = 0.0012 ng) to make spike-ins' mixture for each Malaise-trap sample.

897 The sum of the two spike-ins: 0.0012 ng + 0.0108 ng = 0.012 ng, and their ratio was:
898 0.0012:0.0108 = 1:9.

899 We used the same spike-in mass for all the Malaise-trap samples except for the 17
900 samples that had already been extracted. For the selected 7 samples used in this
901 study, lysis buffer (500 µl, 350 µl, 245 µl, 171.5 µl, 120 µl and 84 µl) from each sample
902 was transferred into a clean 1.5 ml tube, and the spike-in DNA was added and
903 vortexed for 10 sec. We then extracted DNA with the Qiagen QIAquick PCR purification
904 kit, following the manufacturer instructions. DNA was eluted with 200 µl of elution
905 buffer. In this way, the spike-in DNA was co-purified, co-amplified, and co-sequenced
906 along with the sample DNA (Figure 5). We also recorded the total lysis buffer volume of
907 each sample, for downstream correction.

908 *4 Primer design*

909 For this study, we simultaneously tested two methods for extracting abundance
910 information: spike-ins and UMIs (Unique Molecular Identifiers). UMI tagging requires a
911 two-step PCR procedure, first using tagging primers and then using amplification
912 primers (Figure 6). The tagging primers include (1) the Leray-FolDegenRev primer pair
913 to amplify the 313-bp COI amplicon of interest, (2) a 1- or 2-nucleotide heterogeneity
914 spacer on both the forward and reverse primers to increase sequence entropy for the
915 Illumina sequencer, (3) the same 6-nucleotide sequence on both the forward and
916 reverse primers to 'twin-tag' the samples for downstream demultiplexing, (4) a 5N
917 random sequence on the forward primer and a 4N random sequence on the reverse
918 primer (9N total) to act as the UMI tags for across-species abundance estimation, (5)
919 and parts of Illumina universal adapter sequences to anneal to the 3' ends of the
920 forward and reverse primer regions for the second PCR. By splitting the 9N UMI into
921 5N + 4N over the forward and reverse primers, we avoid primer dimers. The
922 amplification primers include (1) the annealing primer pair to bind to the amplicons of
923 the first PCR, (2) the full length of the Illumina adapter sequences. For further
924 explanation of the design of the tagging primers (except for the UMI sequences), see
925 Yang et al. (2021).

926 *5 PCR and the Begum pipeline*

927 We performed a two-step PCR (Lundberg et al. 2013).

928 The first PCR amplifies COI and concatenates sample tags and UMIs and runs for only
929 two cycles using KAPA 2G Robust HS PCR Kit (Basel, Roche KAPA Biosystems). We
930 used the mlCOIintF-FolDegenRev primer pair (Yu et al. 2012; Leray et al. 2013), which

931 amplifies a 313-bp fragment of the COI barcode; and we followed the *Begum* protocol
932 (Zepeda-Mendoza et al. 2018, Yang et al. 2021), which is a wet-lab and bioinformatic
933 pipeline that combines multiple independent PCR replicates per sample, twin-tagging
934 and false positive controls to remove tag-jumping and reduce erroneous sequences.
935 Twin-tagging means using the same tag sequence on both the forward and reverse
936 primer in a PCR. We performed 3 PCR replicates per sample, which means we used 3
937 different twin-tags to distinguish the 3 independent PCR replicates. *Begum* removes
938 erroneous sequences by filtering out the sequences that appear in a low number of
939 PCR replicates (e.g. one) at a low number of copies per PCR (e.g. 4 copies), because
940 true sequences are more likely to appear in multiple PCRs and with high copy
941 numbers. The 20 µl reaction mix included 4 µl Enhancer, 4 µl Buffer A, 0.4 µl dNTP (10
942 mM), 0.8 µl of 10 mM forward primer, 0.8 µl of 10 mM reverse primer, 0.08 µl KAPA 2G
943 HotStart DNA polymerase (Basel, Roche KAPA Biosystems), 5 µl template DNA and 5
944 µl water. PCR conditions were initial denaturation at 95°C for 3 minutes, followed by
945 two cycles of denaturation at 95°C for 1 minute, annealing at 50°C for 90 seconds, and
946 extension at 72°C for 2 minutes. Then the products were purified with 14 µl of KAPA
947 pure beads (Roche KAPA Biosystems, Switzerland) to remove the primers and PCR
948 reagents and were eluted into 16 µl of water.

949 The second PCR amplifies the tagged templates for building the libraries which can be
950 sequenced directly on Illumina platform. The 50 µl reaction mix included 5 µl TAKARA
951 buffer, 4 µl dNTP (10 mM), 1.2 µl of 10mM forward primer, 1.2 µl of 10mM reverse
952 primer, 0.25 µl TAKARA Taq DNA polymerase, 15 µl DNA product from the first PCR,
953 and 23.35 µl water. PCR conditions were initial denaturation at 95°C for 3 minutes, 5
954 cycles of denaturation at 95°C for 30 seconds, annealing at 59°C for 30 seconds (-1 °C
955 per cycle), extension at 72°C for 30 seconds, followed by 25 cycles of denaturation at
956 95°C for 30 seconds, annealing at 55°C for 30 seconds, extension at 72°C for 30
957 seconds; a final extension at 72°C for 5 minutes, and cooldown to 4°C.

958 From all second PCR products, 2 µl was roughly quantified on 2% agarose gel with
959 Image Lab 2.0 (Bio-Rad, USA). For each set of PCR reactions with the same index,
960 amplicons were mixed at equimolar ratios to make a pooled library. One PCR negative
961 control were set for each library. We sent our samples to Novogene (Tianjin, China) to
962 do PE250 sequencing on Illumina NovaSeq 6000, requiring a 0.8 GB raw data from
963 each PCR reaction.

964 *6 Bioinformatic processing*

965 *AdapterRemoval* 2.1.7 was used to remove any remaining adapters from the raw data
966 (Schubert et al. 2016). *Sickle* 1.33 was used to trim away low-quality bases at the

967 3'ends. *BFC* v181 was used to denoise the reads (Li 2015). Read merging was
968 performed using *Pandaseq* 2.11 (Masella et al. 2012). *Begum* was used to demultiplex
969 the reads by sample tag and to filter out erroneous reads
970 (https://github.com/shyamsg/Begum, accessed 07 Sep 2021). We allowed 2-bp primer
971 mismatches to the twin-tags while demultiplexing, and we filtered at a stringency of
972 accepting only reads that appeared in at least two PCRs at a minimum copy number of
973 4 reads per PCR, with minimum length of 300 bp. This stringency minimized the false
974 positive reads in the negative PCR control. *vsearch* 2.14.1 (Rognes et al. 2016) was
975 used to remove chimeras (`--uchime_denovo`). *Sumaclust* 1.0.2 was used to cluster
976 the sequences into 97% similarity OTUs. The python script tabulateSumaclust.py from
977 the DAMe toolkit was used generate the OTU table. Finally, we applied the R package
978 LULU 0.1.0 with default parameters to merge oversplit OTUs (Frøslev et al. 2017). We
979 also removed any OTUs in which we found stop codons. The OTU table and OTU
980 representative sequences were used for downstream analysis.

981 Begum removed UMIs while sorting tags. Because of our complicated primer structure,
982 there is no software available for our data to count the number of UMIs per OTU. We
983 wrote our own bash scripts to process data from the Pandaseq-merged files, which
984 includes all the UMIs, tags, and primers. We first used *Begum*-filtered sequences as a
985 reference to filter reads in each PCR set, and put the UMI information on the read
986 headers. Then we carried out reference-based OTU clustering for each PCR with
987 Qiime 1.9.1(`pick_otus.py -m uclust_ref -s 0.99`), using the OTU
988 representative sequences as the reference, counted UMIs and reads for each OTU in
989 each PCRset, and generated the UMI and READ OTU tables.

990